ABSTRACT

HWANG, JEESANG. Carbon Black Filled Electrospun Fiberweb: Electrical and Mechanical Properties. (Under the direction of Tushar K. Ghosh and John F. Muth)

The development of flexible and compliant conductive polymer composites with "textile" like characteristics remains an important endeavor in light of the recent activity in polymer/textile based electronics. In the present work, electrospinning is used to prepare a composite fiber containing carbon black (CB) and polyurethane (PU). The effects of introducing CB into the PU-matrix in the form of fiberweb have been investigated in terms of mechanical, electrical, and thermal properties. A percolation behavior of the CB filled fibers has been investigated using simulation. Theoretical percolation threshold was determined at CB volume fraction of 9.3. The highest conductivity of the fiberweb was experimentally determined to be $\sim10^{-2}$ S/cm for 8.03 vol% of CB filler content, which is deemed useful for a number of applications including electrodes in poymer actuators. However percolation threshold of the conductivity of the PU-CB electrospun fiberweb was experimentally determined to be between 4.6-5.0 vol% of CB. The discrepancy may be due to the idealized structure assumed in the simulation. The critical exponent of percolation (t) was calculated as 2.165, when the percolation threshold was assumed to be at 4.6 vol%.

Electrical and mechanical properties of the fiberwebs have been compared with films with same constituents. The current-voltage (I-V) relationship of both spin-cast films and electrospun fiberweb was studied to understand the mechanism of electrical conduction. In both cases, at high absolute values of voltage the current increased linearly, while for low voltages the current values are substantially lower, as a result the behavior resembled like diodes. On subsequent voltage sweeps, lower resistance values were recorded and the

relationship became more linear over the whole voltage range. The data suggests alteration of the initial percolation network on application of high voltage. This non-Ohmic behavior is attributed to quantum tunneling conduction mechanism. The results seem to confirm the tunneling-percolation behavior of the CB-PU composite fiberweb investigated in this research. Generally, fiberwebs show better electrical and mechanical properties than the films. Electrical conductivity of the fiberwebs is generally higher than the films.

As expected, elastic modulus of fiberwebs is found to be much lower than the films. The increase in bond density and the overall area of the bonds for higher CB content as well as the reinforcement effect of high modulus CB particles are likely to improve the modulus of the fiberweb. Both films and fiberwebs show similar piezoresistive behavior, however gauge factor of fiberwebs are slightly higher than equivalent films. To demonstrate a potential use, the CB-PU nanocomposite fiberweb was applied in the form of flexible electrodes on a circular dielectric elastomer actuator. The maximum mean areal actuation strain of 12.74% was recorded with 5.58 vol% carbon black filled fiberweb as electrodes applied on and VHB-4910 acrylic films.

CARBON BLACK FILLED ELECTROSPUN FIBERWEB:

ELECTRICAL AND MECHANICAL PROPERTIES

by

JEE SANG HWANG

A dissertation submitted to the Graduate Faculty of

North Carolina State University

in partial fulfillment of the

requirements for the degree of

Doctor of Philosophy

FIBER AND POLYMER SCIENCE

Raleigh, NC

2006

Approved by

Dr. C. M. Balik	Dr. J. F. Muth

Dr. T. K. Ghosh	Dr. R. Kotek
Chair of Advisory Committee	Co-chair of Advisory Committee

Dedicated to my parents,

my wife, Kyeong Pang, and my son, Ethan.

BIOGRAPHY

JEESANG HWANG was born on January 1, 1973 in Seoul, Korea. He attended Mapo high school in Seoul and graduated in 1991. In February 1999, he graduated from the Soongsil University with a Bachelor of Science degree in Textile Engineering department. He continued study in Textile Chemistry program and obtained his Master of Science in February 2001. In May 2001, he got married to his wife, Kyeong Pang. He first came to United States with his wife in July 2001. After one year, he enrolled in North Carolina State University in Fiber and Polymer Science program where he worked towards his Doctor of Philosophy degree. He got his son, Ethan in September 2003.

ACKNOWLEDGEMENTS

TABLE OF CONTENTS

vi

LIST OF FIGURES

LIST OF TABLES

CHAPTER 1. INTRODUCTION

Fibers can be made from almost any material such as glass, ceramic, polymer and metal. Fibers are used in diverse areas either by themselves in interwoven or interlaced form or as reinforcement for other materials. Most polymeric fibers are highly flexible, quite elastic and lightweight and are therefore best suited for textile products. On the other hand, carbon fibers are electrically conductive, tougher and stronger than most polymer fibers [1] and are used in applications where electrical conductivity and stiffness are important, e.g. static dissipation, or as reinforcement of composites.

Composites are a class of engineering materials consisting of a mixture of two or more components to produce a multiphase system with different physical properties obtained from the constituents [2]. In carbonaceous composites, one of the phases is carbon, in some form, and it is generally introduced to impart certain functionality or to improve a certain behavior of the composite. Carbonaceous composite fibers or carbon filled polymeric fibers generally have improved electrical and mechanical properties due to the incorporation of the carbon particles on the surface or into directly fiber. The carbonaceous composite fibers can be used in many applications such as static dissipation [3], electromagnetic shielding [4], and radio frequency interference [5],

where low to moderate conductivity is acceptable. The enhanced mechanical properties can be useful in applications such as aerospace and defense where weight and mechanical properties are critical.

The interest in carbon filled polymeric materials including fibers have been renewed with the advent of nanoparticles such as carbon nanotubes for use as multifunctional material due to its remarkable electrical, thermal and mechanical properties. Additionally, with these additives composite properties can be significantly enhanced at much lower loadings [6, 7]. Among the available fillers, carbon black (CB) and carbon nanotubes (CNT) have been used extensively due to their ability to impart high electrical conductivity to a polymer matrix at relatively low filler content [6-9]. CB has been used widely in conventional polymer composites due to their relative advantages of low cost, small particle size (high surface area), and aggregation behavior. CB filled polymer composites in film form have been investigated for various applications including sensors [10], electrodes [11], and electromagnetic interference shielding [12]. However, investigation of CB/polymer composite behavior in fiberweb form has been very limited. In general, use of fiberwebs may be desirable for some applications because of their porosity, lighter weight, and relatively more flexibility.

In this work, electrospinning has been utilized to fabricate a flexible and conductive

fibrous network. Electrospinning is a simple process for forming nanoscale to microscale fibers with diameters ranging from tens of nanometers to microns. It has been used recently to fabricate the nanocomposite fiberwebs with various fillers such as CNTs [13, 14], and nanoclays [15]. However, there are no published report on electrical characteristics of electrospun fiberwebs filed with CBs.

The study reported here presents electrical and mechanical behavior of CB filled polyurethane (PU) composite fiberwebs fabricated using electrospinning. In addition, to demonstrate its use as a conductive layer, the composite fiberweb has been evaluated as electrodes for dielectric electroactive actuators (DEA).

1.1. Objective of Research

The primary objective of this research is to study the characteristics of CB/PU electrospun fiberwebs for their electrical and mechanical properties relevant to self-monitoring layer compatible with textile products.

Second objective of this research is to explore the comparative advantage (or lack of) of electrospun fiberweb over thin films.

To reach this goal, the following research tasks need to be completed:

- Fabricate the PU/CB composite fiberweb via electrospinning.

- Investigate percolation threshold of PU/CB electrospun fiberweb via experiments and simulation.

- Examine relevant electrical and mechanical properties of the composite fiberwebs.

- Fabricate the PU/CB composite films via spin-casting.

- Evaluate electrical and mechanical properties of the composite films.

- Evaluate composite fiberwebs as flexible electrodes for DEA.

1.2. Organization of the Dissertation:

The dissertation is written in the form of three research papers, to be published in appropriate refereed journals. The section 2 entitled Background covers detailed discussion of published relevant literature beyond the scope of the papers. The Conclusion section covers all of the work. The Appendices provide further details of methods that may have been used or details of data that had to be excluded from the papers for brevity. Needless to say that this has resulted in some redundancy of information. In addition, it should be noted that particle contents of the composites investigated in this research are expressed inactual vol% (as determined by TGA, section 4.4.3), unless explicitly noted as nominal.

1.3. References

1.   Astrom, B.T., *Manufacturing of Polymer Composites.* 1997: p. 96.

2.   *Encyclopedia of composite materials and components.* 1986.

3.   Maclaga, B., and Fisher, W. K., *Static Dissipation Mechanism in Carpets Containing Conductive Fibers.* Text. Res. J., 2001. **71**(4): p. 281.

4.   Dhawan, S.K., Singh, N., Rodrigues, D., *Electromagnetic Shielding Behaviour of Conducting Polyaniline Composites.* Sci. Technol. Adv. Mat., 2003. **4**: p. 105.

5.   Heiser, J.A., King, J. A., Konell, J. P., and Sutter, L. L., *Shielding Effectiveness of Carbon-Filled Nylon 6,6.* Polym. Compos., 2004. **25**(4): p. 407.

6.   Huang, J., *Carbon Black Filled Conducting Polymers and Polymer Blends.* Adv Polym Technol, 2002. **21**: p. 299.

7.   Chung, D.D.L., *Review Electrical Applications of Carbon Materials.* J Mater Sci, 2004. **39**: p. 2645.

8.   Munoz, E., Suh, D., Collins, S., Selvidge, M., Dalton, A. B., Kim, B. G., Razal, J. M., Ussery, G., Rinzler, A. G., Martinez, M. T., and Baughman, R. H., *Highly Conducting Carbon Nanotube/Polyethylene Composite Fibers.* Adv Mater, 2005. **17**: p. 1064.

9.   Seoul, C., Kim, Y., and Baek, C., *Electrospinning of Poly(vinylidenefluoride)/Dimethylformamide Solutions with Carbon Nanotubes.* J Polym Sci, Part B: Polym Phys, 2003. **41**: p. 1572.

10.   Chen, S.G., Hu, J. W., Zhang, M. Q., Rong, M. Z., and Zheng, Q., *Improvement of Gas Sensing Performance of Carbon Black/Waterborne Polyurethane Composites: Effects of Crosslinking Treatment.* Sens Actuators, B, 2006. **113**: p. 361.

11.   Richner R, M.S., Wokaun A, *Grafted and Crosslinked Carbon Black as an Electrode Material for Double Layer Capacitors.* Carbon, 2002. **40**: p. 307.

12.   Bigg DM, S.D., *Plastic Composites for Electromagnetic Interference Shielding Applications.* Polym Compos, 1983. **4**: p. 40.

13.   Dror, Y., Salalha, W., Khalfin, R. L., Cohen, Y., Yarin, A. L., and Zussman, E., *Carbon Nanotubes Embedded in Oriented Polymer Nanofibers by Electrospinning.* Langmuir, 2003. **19**: p. 7012.

14.   Salalha, W., Dror, Y., Khalfin, R. L., Cohen, Y., Yarin, A. L., and Zussman, E., *Single-Walled Carbon Nanotubes Embedded in Oriented Polymeric Nanofibers by Electrospinning.* Langmuir, 2004. **20**: p. 9852.

15.   Hong, J.H., Jeong, E. H., Lee, H. S., Baik, D. H., Seo, S. W., and Youk, J. H., *Electrospinning of Polyurethane/Organically Modified Montmorillonite Nanocomposites.* J Polym Sci, Part B: Polym Phys, 2005. **43**: p. 3171.

CHAPTER 2. BACKGROUND

2.1. Introduction

Nanocomposites are a special class of composite materials in which one of the components is a nanoscale material. They often have properties that are superior to conventional microscale composites and can be synthesized using surprisingly simple and inexpensive techniques. Typically, nanocomposites are nanoparticles dispersed in polymer, metal or ceramic matrix. Inclusion of nanoparticles in polymer or other matrices can result into novel properties not seen with materials of higher scale. These unique properties include enhanced electrical property [1, 2] with low percolation threshold, and improved mechanical properties with little effects on ductility of the polymer [3, 4], optical [5], and thermal properties [6, 7]. Excellent examples of nanocomposites are found in nature also. The abalone shell, for example, has alternating layers of calcium carbonate and a rubbery biopolymer. It is much stronger and tougher than many man-made materials [8].

Nanoparticles are ultrafine particles of nanometer dimensions and show size dependency on the properties of composites [9]. In general, nanoparticles have large number density of particles per unit volume of matrix, short distances between particles,

and posses very high surface to volume ratio. In composites fillers with higher surface area are generally more effective. Therefore, with nanoparticles it is possible to achieve comparable composite properties at much lower loading of filler. In recent years, nanocomposite materials have been studied very widely due to the synergistic properties of two or more components. Specifically polymer materials have been filled with several nanoparticles in order to improve properties like heat resistance, mechanical properties, electrical properties, barrier properties, and optical properties. Such enhancements are due to the physical presence of the nanoparticle and to the interaction of the polymer with the particle and the state of dispersion [10]. A well dispersion state of nanoparitcles can be obtained by means of chemical modifications [11] and non-chemical modifications [12]. Properties of composites that have been shown to undergo substantial improvements due to incorporation of nanoparticles include:

- Mechanical properties, e. g. strength, modulus and dimensional stability
- Decreased permeability to gases, and moisture
- Thermal stability
- Flame retardancy and reduced smoke emission
- Chemical resistance
- Surface appearance
- Electrical conductivity
- Optical clarity in comparison to conventionally filled polymers

It is also important to recognize that nanoparticle inclusion produces significant property improvements with relatively low loading levels. Generally, traditional microparticle additives require much higher loading levels to achieve similar performance. This in turn can result in significant weight reductions (of obvious importance for various military and aerospace applications) for similar performance.

2.2. Carbonaceous Material Filled Nanocomposite Fiber

For the nanocomposite fibers, carbon nanotubes (CNTs) have been usually used for the reinforcing material of a polymeric fiber. Other than CNT, graphite and nanoclay have been also used for a nanocomposite fiber as a filler material. Table 1.1 shows the summery of nanocomposite fibers. From these studies, it has been found that there are lack of reports about CB filled composite fiber and property enhancements of nanocomposite fibers include strength, stiffness, thermal stability, electrical and thermal conductivity as well as optical anisotropy.

Table 2.1. Summary of nanocomposite fibers, continued page 11-12.

Polymer	Filler	Spinning	Event	Ref.
PVA	SWNT	Gel spinning	40% increase of modulus of the PVA/SWNT (3wt% of SWNT) - not because of crystalinity, but SWNT in amorphous region	[13]
UHMWPE	MWNT	Gel spinning	Functionalization of MWNT by oxidation - carboxyl groups on the surface of MWNT - mechanical and thermal property improved	[14]
PAN	SWNT	Gel spinning	Modulus of PAN/SWNT(10wt%) increased twice compared to control sample - interaction between PAN/SWNT improved - broadening of the tanδ peak to higher temperature Improved solvent resistance	[15]
PEI	SWNT	Gel spinning	Affinity of PEI and amine into SWNT - shift of T_g - similar Raman spectra between SWNT and PEI/SWNT fiber Electrical conductivity: 100 to 200 Sm^{-1}	[16]
Polyimide	SWNT	Melt spinning	Improved tensile property due to the alignment of SWNTs in the fiber	[17]

Table 2.1. Summary of nanocomposite fibers, continued page 11-12.

Polymer	Filler	Spinning	Event	Ref.
PLA/PAN	SWNT	Electro-spinning	Incorporation of SWNTs in the fiber confirmed by Raman spectroscopy - estimate diameter of SWNT	[18]
PS/PU	SWNT	Electro-spinning	Ester functionalized SWNT improve mechanical property	[19]
PAN	MWNT	Electro-spinning	Tensile modulus increased with 20wt% MWNT Tensile strength increased with 5wt% MWNT, then decreased due to poor dispersion and poor interfacial contact of MWNT	[11]
PVDF	SWNT	Electro-spinning	Percolation threshold 0.003 wt%	[20]
PMMA/PEO	CB	Electro-spinning	Color change in CB filled electrospun web	[21]
PAN	GNP	Electro-spinning	Improved thermal and mechanical property	[22]
PU	MMT	Electro-spinning	Improved tensile modulus and strength	[23]

Recently nanocomposite fibers have been fabricated by using electrospinning technique. Carbon nanoparticles such as carbon nanotubes, carbon blacks, and graphite nanoplatelets can be incorporated into the fiber via the in-situ spinning. Out of these materials, carbon nanotubes have been of interest in the nanocomposite fiber technology due to its superior fineness, mechanical, electrical and thermal property. Moreover it is expected to align the nanotubes during the electrospinning process due to the sink flow and the high extension of the electrospun jet [12]. Therefore most of the electrospinning with the carbon nanotubes are related with the alignment or the orientation of the nano tube assemblies in the fiber [11, 12, 18, 24-26]. If enough alignment is achieved, the fiber will start to display some of the properties of the nanoparticles such as low electrical and thermal resistivity and high tensile strength. Consequently these composite fibers provide advantages in conductivity, weight savings, flexibility, and durability. These advantages have led to increasing interest in applying composite fibers in industrial applications.

2.3. Electrospinning

Electrospinning is a simple process for forming nanofibers with diameters ranging from tens of polymeric fibers to microns [27, 28]. Conventional fiber spinning

techniques, e. g. melt spinning, dry spinning or wet spinning, depend on mechanical forces to produce fibers by extruding polymer melt or solution through a spinneret and drawing the obtained filaments as they solidify. Electrospinning uses a fundamentally different approach to fiber production by applying electrostatic forces to the fiber spinning process, that is, a high voltage to the polymer solution or melt. Electrospinning has been known since 1934 by Formhals [29], but its significance for making nanofibers was recognized recently. In 1969, Taylor [30] reported that the effect of an electric field on the geometry of a viscous liquid droplet suspended at the end of a capillary. The conical shape of the liquid droplet was observed when the applied electric field surpasses the surface tension of the liquid droplet. This conical shape of the droplet was called "Taylor Cone". In 1971, Baumgarten [31] reported the electrospinning of acrylic microfibers whose diameters ranged from 500 to 1,100 nm. Baumgarten determined that solution parameter such as viscosity is related to the morphology of the fiber. After a few decades, in depth study of electrospinning has been carried out by Doshi and Reneker [27]. They provide the nanofibers having diameters in the range of 50 nm to 5 μm by electrospinning from PEO (Mw = 145,000 g/mol) solutions. They concluded that as the polymer concentration increases, the solution viscosity increases, thus higher voltage is required to the electrospinning process. After few years, electrospinning has

14

been studied in various forms of applications because of the attractive properties of nanofibers. Although the process of electrospinning has been known for over half a century, the current understanding of the process and those parameters are very limited. Therefore, there are requirements for the many processing parameters, influence the spinnability and physical properties of nanofibers, including solution concentration, surface tension of the solution, surface charge density, and electric filed etc.

In the electrospinning process, a polymer solution is held in the syringe and forms droplet at the end of capillary by its surface tension. Then, a polymer solution is subjected to an electric field. A high electric field is used to induce the charges on polymer solution. When an external electric field is applied to a polymer solution, ions in the solution will be aggregated around the electrode of opposite polarity. Positive ions are getting close to the negatively charged electrode and negative ions are getting close to the positively charged electrode. This results in excess of charge of opposite polarity in the solution near an electrode. Therefore, positive surface charges are generated on the surface of the droplet that is hanged at the end of capillary. Then, like charges generate repulsive forces, cause force directly opposite to the surface tension of the liquid surface, within induced charge distribution. This results in the drop to distort into the shape of a cone. As the electric field is increased, the hemispherical surface of

the solution at the tip of the capillary tube elongates to form a conical shape known as the Taylor cone [30]. When the electric field reaches a critical value at which the repulsive electric force overcomes the surface tension, a charged jet of the polymer solution is ejected from the tip of the Taylor cone and travel toward the nearest electrode of opposite polarity. The electrically charged jet undergoes a series of electrically induced bending instabilities, cause whipping motion and break up the jet, during its passage to the collector. As the jet diameter decreases, the surface charge density increases. The high repulsive forces from the increased charge density split the jet. These two motions make jet stretch and form of ultra thin fiber. Also, this stretching process is accompanied by the rapid evaporation of the solvent molecules. Ultra fine fibers can be obtained by combining this two-process. The dry fibers are accumulated on the surface of the collection screen resulting in a nonwoven electrospun web.

Because of the outstanding advantages of electrospun fiber and web such as high aspect ratio and fine diameters, electrospun webs can be widely applied to various applications such as filters [32], tissue engineering scaffolds [33], optical sensors [34], super hydrophobic surfaces [35], and electrodes in supercapacitors [36]. A fiber of nano-scale diameter has significantly higher surface area compared to a conventional fiber. Consequently, the fiber aspect ratio (L/D) may significantly increase as the

diameter of the fiber decreases to nano-scale. Therefore, the web produced from electrospinning has small pore size and high efficiency of filtration. In the area of the composite, higher strength and larger surface area are very useful for the bonding or strength between fiber and matrix. In the biomaterial applications, larger surface area provides higher chemical reactivity that enables filtering and detection of molecules.

2.4. Carbon Black

Carbon black is an amorphous form of carbon with a structure similar to disordered graphite [37]. When aromatic hydrocarbons are placed to incomplete combustion of natural gases at high temperature, their molecules will dissociate through the rupture of C-H bonds. Carbon atoms and aromatic radicals continuously react to form layer structures composed of hexagonal carbon rings, which tend to stack in three to four layers, forming crystallographic structures. Crystallites then form primary particles, which further form into primary aggregates. Van der Waals forces cause these aggregates to join in agglomerates. Within the carbon black primary particles, electron can flow though the highly conjugated carbon bonding present in the crystalline regions of the carbon particle when external forces are subjected to the particle. Within the aggregates of primary particles electrons can flow along the conjugate bond.

Consequently electrical conductivity can be shown in the carbon black particle.

Based on X-ray diffraction study, Warren [38] proposed that carbon blacks are composed of small layers with the same atomic positions as graphite within the layers. Franklin [39] showed that the various types of carbon differ only in the magnitude of their variation from graphite rather than different crystallographic structure. Sweitzer *et al*. [40] proposed the model that carbon black particles consists of many small pseudographitic crystallites located within the particle. A certain percentage of amorphous or disordered material is present in the spaces between the crystallites. These crystallites consist of two to five layers of hexagonally packed carbon atoms in random orientations. Therefore, property of carbon blacks can be directly related with the graphite crystal. The graphite crystal consists of stacks of multi layers of carbon atoms separated by a spacing of 0.34 nm. The carbon atoms within the layer are linked together by covalent bonds having strengths of 400 kJ/mol. These strong bonds are the major factors of the extremely strong and stiff nature of the graphite structure in plane. However, the strength of c-axis direction is relatively low due to weak van der Waals bonds between the layers [41]. This explains the poor compressive properties of crystalline graphite due to low shear resistance. These characteristics of the graphite, also, affects on the electrical property of the carbon black since carbon blacks are

composed of graphite layers [42]. Natural graphite single crystals behave as semi-metal

due to the anisometry of the electrical behavior between a-axis and c-axis. For example,

the specific resistance of graphite single crystals is about 5×10^{-5} ohm-cm in the a-axis

direction while c-axis directions shows about 10^4 higher resistance [42]. Therefore

primary particle of the carbon black can be considered as semi-metal, however, it is

usually regarded as a promising conducting material because of forming agglomerations.

The micro structural model by Sweitzer *et al.* [40] are illustrated in Figure 2.1 in

comparison to hexagonal graphite. Figure 2.1 (a) depicts the random orientation of

crystallites within a single carbon black particle and a typical crystallite is illustrated in

Figure 2.1 (b). The unit cell of the graphite is illustrated in Figure 2.1 (c).
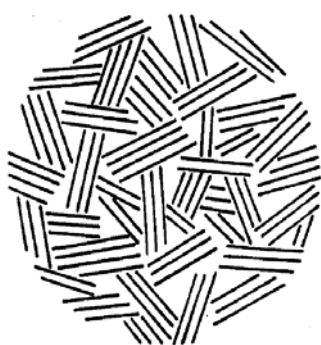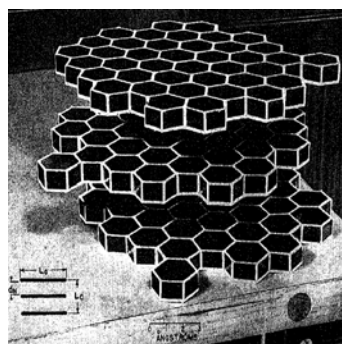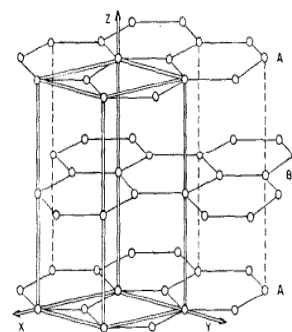
(a)   (b)   (c)

Figure 2.1. Models for carbon black micro structures [40] in comparison to graphite [43]. (a) model crystallites in carbon black particles (b) scale model of carbon black crystallite (c) unit structure of hexagonal graphite unit.

Morphology of the carbon black shows that carbon black consists of prime particles fused into primary aggregates [44, 45]. The particle size, aggregate size and shape of the carbon black primary particle determine the structure of carbon black. Medallia [45] further suggested that smaller particles have higher inter-aggregate attractive forces, resulting into a high secondary structure and an increased agglomerate size. If the aggregates are composed of few prime particles, carbon black is designated a low structure carbon black. A high structure carbon black consists of relatively many prime particles. A high structure carbon black easily forms agglomerates which mean that the dispersion process should require more energy to separate them. Since high structure carbon blacks tend to produce larger aggregates than low structure blacks and are separated by smaller distances, this phenomenon lead to higher conductivity at the same loading of low structure carbon black [46-48]. Figure 2.2 shows the model of carbon black structure: the lower structures are more spherical. For high structure carbon black, the gap width between agglomerates is much smaller than the low structure carbon black. Polley *et al.* [49] reported that when the separation distance between aggregates

is less than some critical distance, electrons can flow across the polymer barrier and a high conductivity is generated. In view of this, high structure carbon black can generate electrical conductivity by a continuous path within the agglomerate and/or a small distance, which is denoted as tunneling distance. Due to the tunneling, its conductivity may increase with much lower loading of carbon black than with low structure carbon black. Different resistivity behaviors of carbon black filled composites are described in Figure 2.3. Two types of carbon blacks were used as a conductive filler: Ketjenblack (high structure), ECF black (electric conductive furnace black, low structure) [50]. Ketjenbalck filled polymer composite shows much lower percolation threshold than ECF black filled polymer composite.
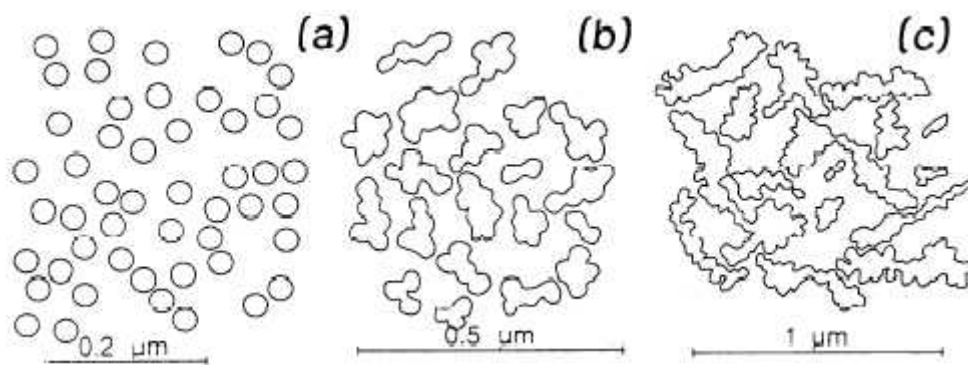
Figure 2.2. Schematic descriptions of composites made of carbon blacks. (a) low structure (b) intermediate structure (c) high structure [46].
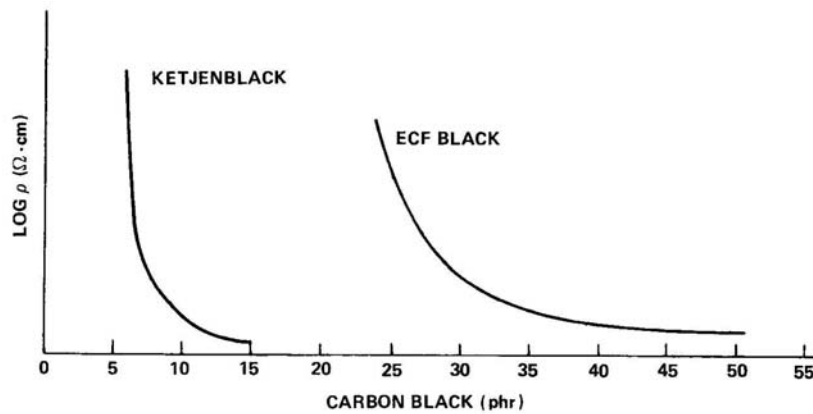
Figure 2.3. Dependence of the resistivity on carbon black loading for a Ketjenblack, and a ECF black [50].

2.5. Percolation Mechanism in Carbon Black Filled Composite

The electrical conduction in conductive filler loaded composite is mainly determined by two mechanisms, percolation in a continuous conductive network [51, 52] and/or quantum tunneling between isolated conductive particles [53-55].

In continuous network conduction, a percolation transition is only happened at when conductive particles are in direct contact. One of the good examples for the first case is metal-insulator composites [51, 56]. For some granular metals, percolation transition is due to the coalescence of metallic particles. Below percolation threshold, particle agglomerates are not forming continuous networks but isolated in polymer matrix;

therefore, no conduction network forms below the percolation threshold. Percolation theory approach to conduction in random media has been studied by Kirkpatrick [52]. He found, that when the volume fraction of the conducting component exceeds the critical volume fraction, the dependence of conductivity of the mixture of conducting and non-conducting component could be described by a power law relation. This relation shows a reasonable agreement with the experimental data on granular metals [51]. Moreover, the conductivity exponent was found to be very close to the predicted universal value of $t \cong 2.0$. However, some discrepancies between values of the critical exponents have been reported [46, 57-60]. This difference shows that the conductivity exponent for continuum percolation systems is non-universal and required to consider other factors such as particle size and structure, tunneling distance and cluster structure. Therefore, there still remain numerous pending questions that can depart from the percolation theory.

As the carbon particles approach each other, current can flow even though there are no direct contacts between carbon particles. This mechanism is called 'quantum mechanical tunneling', where electrons can move through the insulator between conductive elements with a certain probability [61]. In other words, electrons can hop from conductor to conductor by "tunneling" through the insulating barrier.   Figure 2.4

describes a simple insulator barrier having energy V_0 and a width w. In classical

mechanics approach, no particles will be observed to the right side of the barrier unless

they have a kinetic energy E greater than V_0. On the other hand, if particles obey the

quantum mechanics, a small fraction of particles can be observed to the right side of the

barrier due to the wave nature of the electrons. The characteristic length of the barrier

width can be calculated by using the equation below [62]

$$\delta = \frac{h}{2\pi\sqrt{2m(V_0 - E)}}$$

(1.1)

where h is Planck's constant, m is the electronic mass, V_0 is the potential barrier energy,

and E is the kinetic energy. Then, δ is the order of 1 Å, so that tunneling current can be

observed only for very thin barrier widths.
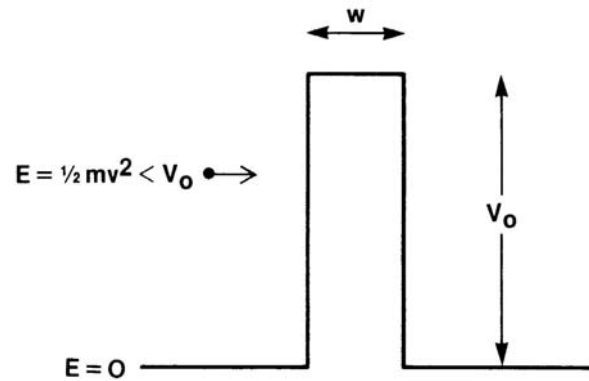
Figure 2.4. Schematic diagram of a potential barrier of height V_0 and width w with a particle of kinetic energy E [63].

This electron transport mechanism by tunneling can be well verified by the temperature dependence of the resistivity of carbon black polymer composites at T > 100K [53, 54, 64, 65]. When the temperature is raised, the volume of the polymeric insulator expands, that is, the thermal expansion of the polymeric material widens the gap between two conductive materials [65]. Widen gap can transform the electrical property of composite from conductive to non-conductive materials since insulating gap between conductive particles can be expanding over the tunneling distance. However, this raised temperature results in thermal fluctuations that can lower the potential barrier energy between two conductive materials. Then it is easier to pass the electrons through

the barrier that has low energy. Thus, the tunneling current can increase at high temperatures.

Many researches have focused on the effect of conductivity of the conductor-insulator composite on the tunneling conduction [46, 47, 54, 58, 60, 61, 65, 66]. Sheng *et al*. [54] presented that fluctuation-induced tunneling accounts for the electrical conductivity of the carbon black-PVC composites and thermal fluctuations plays an important role in determining the dependence of the conductivity on temperature and electric field. They calculated tunneling current with the equation given by:

$$j(\varepsilon) = j_0 \exp\left[-\frac{\pi \chi w}{2}\left(\frac{\varepsilon}{\varepsilon_0} - 1\right)^2 \right], \quad |\varepsilon| < \varepsilon_0 \qquad (1.2)$$

where $\chi = \left(\dfrac{2mV_0}{h^2}\right)^{1/2}$, ε is the electric field in the gap, m is the electron mass, $\varepsilon_0 = \left(\dfrac{4V_0}{ew}\right)$, and V_0 is the potential barrier and w is the gap width. In this equation (1.2), width of the tunneling barrier was assumed as 75 Å. This relation is based on the exponential dependence of the tunneling current on the gap width. In 1957 Polley *et al*. [49] proposed that electrons jump across the gap with an exponential dependence on gap width. Recently Balberg [46] reported that there is an exponential decay of the

tunneling conductance with the distance between two conductive particles. The tunneling conductance, g, between two conductive particles separated by a distance r is given by

$$g = g_0 e^{-r/d} \qquad (1.3)$$

where g_0 is a constant, and d is the characteristic tunneling distance. The characteristic tunneling distance has been reported typically of the order of tens of angstroms [46, 50, 54, 61]. Sherman [61] reported that electrons can tunnel quantum mechanically between conductive elements when proximity between two conductive particles is small (≤ 100 Å). Medalla [45] reported that tunneling distance may be of the order of 15-100 Å. With the use of tunneling distance, connected particles by nearest-neighbor tunneling are described well in Figure 2.5. The black circles represent the carbon particles while their gray shells represent the effective tunneling distance. The nearest-neighbor connections yield a continuous conductive path.
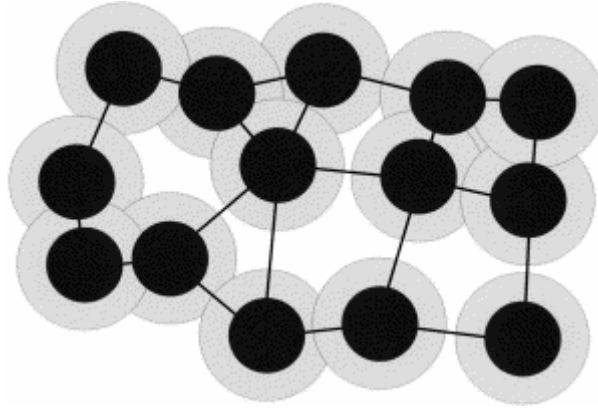
Figure 2.5. An illustration of a close-packed network of low structure carbon particles that are connected by nearest neighborhood tunneling [47].

Balberg [46] used theory of percolation to explain coexistence of a quantum tunneling in a continuous network in the carbon black composites. As the carbon particle loadings increase, filler particles agglomerate and form a conductive network. In some region carbon particles or agglomerates are not forming a continuous path but the distance between carbon particles or agglomerates are getting closer. The larger the volume fraction of carbon particles in the composite, the smaller the average distance between two agglomerates or carbon particles. If the distance is decreased to the tunneling distance of the carbon particles, the electrons can be transported between two carbon particles or agglomerates by quantum tunneling. Thorough the coexistence of a quantum tunneling and percolation, high conductivity in the composite can be explained

even though the loading amount of conductive particles are not sufficient to form a

percolation network.

2.5.1. Percolation Model

The electrical conductivity of mixtures of conductive and insulating materials is

generally dependent on the formation of the conductive network through the medium.

To understand this network formation, many percolation models and equations have

been proposed.

Statistical percolation model basically deals with the probability of particle contacts

within the medium. Two of early percolation models often referenced are the models

proposed by Kirkpatrik [52] and Zallen [67]. A finite regular array of points and bonds

was used to determine the percolation concentration. By computer simulation, it was

possible to predict the points and bonds that were in a cluster, and determine if that

cluster spanned the boundaries of the system. It was then possible to predict the

percolation threshold. The model followed a power law equation of the following form:

$$\sigma = \sigma_c \left(\upsilon - \upsilon_c \right)^t \quad \text{for } v > v_c \qquad (1.4)$$

where σ_c is conductivity of the conducting component, υ is its volume fraction, t is a critical exponent, and υ_c is the critical volume fraction. The values of σ_c depend on the dimensions of the lattice. This particular model, however, was not accurate in determining the percolation threshold.

Bueche [68] proposed a model to explain the S-shaped conductivity curves of binary mixtures on the basis of the Flory concept of polymer gelation. The equation is as follows:

$$\frac{\rho}{\rho_m} = \frac{\rho_f}{(1-V)\rho_f + V\omega\rho_m} \qquad (1.5)$$

where ρ is the resistivity of the mixture, ρ_m is the resistivity of the insulating material, ρ_f is the resistivity of the conductive material, V is the volume fraction of the conductive phase in the mixture, and ω is the fraction of the conductive filler being incorporated in an infinite cluster. The value of ω is determined by the subfactors f and α; α is the probability for the appearance of a contact between neighboring particles, and f is the maximum number of contacts a particle can make with its neighbors. Bueche's theory can account for the different drastic jumps in the conductivity and beyond the percolation concentration.

McLachlan [69] pointed out that percolation theory is limited in that the model is applicable only near the percolation threshold. He showed the reason that critical exponent is not universal and there are obvious deviations from the percolation equation in the experimental data. This can be a problem when dealing with real systems such as carbon black-polymer composites. To address this shortcoming of classical percolation theory, McLachlan suggested using the developed General Effective Media (GEM) equation. The GEM model relates the composite's resistivity or conductivity to the concentration of the various components. The GEM equation written in terms of electrical resistivity is

$$\frac{(1-f)\left(\rho_h^{-1/t} - \rho_m^{-1/t}\right)}{\rho_h^{-1/t} + \left(\frac{1-f_c}{f_c}\right)\rho_m^{-1/t}} + \frac{f\left(\rho_l^{-1/t} - \rho_m^{-1/t}\right)}{\rho_l^{-1/t} + \left(\frac{1-f_c}{f_c}\right)\rho_m^{-1/t}} = 0 \qquad (1.6)$$

where f_c is the critical volume fraction of the low resistance (carbon black) component, or percolation threshold; ρ_l the resistivity of the low resistance (carbon black) phase; ρ_m the resistivity of the composite mixture; ρ_h the resistivity of the high resistance (polymer) phase; f the volume fraction of the low resistance (carbon black) phase; t the exponent. The equation (1.6) can be solved for ρ_m, the resistivity of the composite, if an

arbitrary composite is defined by t, ρ_l, ρ_h, and f_c. The value of the critical exponent t is

obtained from a fitting of the experimental data set, and ranges between 0.68 and 2.8

[70-75]. This GEM equation has been used to predict electrical conductivity, thermal

conductivity and dielectric constant [69, 71-74].

2.6. Piezoresistivity in Composites

The name 'piezo' comes from the Greek word "piezin" which means squeezing.

Combined with resistivity it describes the dependence of electrical resistivity on applied

mechanical strain or stress. Piezoresistivity is one of the most often used transducer

effects, in particular for electromechanical sensors made out of semiconoductors.

Typical applications are pressure sensors, accelerometers, etc. The reason for the

common use of the piezoresistive effect is its simplicity. The most popular sensor using

piezoresistivity is a conventional strain gauge. The resistance change is related to the

strain by a gauge factor. Gauge factor (GF) is defined by the equation below,

$$GF = \frac{\text{relative resistance change}}{\text{relative length change}} = \frac{\dfrac{\Delta R}{R}}{\dfrac{\Delta L}{L}} = \frac{\Delta R}{\varepsilon R}$$

(1.7)

where R is an electrical resistance, L is length of the wire, and ε is strain. Strain of piezoresistive materials produces a relative resistance change. The resistance change is due to the changes in resistivity and dimensional changes. The resistance of single wire with a rectangular cross-section is expressed by the equation below,

$$R = \rho \frac{L}{A}$$

(1.8)

where ρ is resistivity. Differentiating equation (1.8) gives a small change in resistance, which is given by the equation below,

$$dR = \frac{L}{A} d\rho + \frac{\rho}{A} dL - \frac{\rho}{A^2} dA$$

(1.9)

and then dividing by the initial resistance leads to equation (1.10)

$$\frac{dR}{R} = \frac{d\rho}{\rho} + \frac{dL}{L} - \frac{dA}{A} = \frac{\Delta\rho}{\rho} + \frac{\Delta L}{L} - \frac{\Delta A}{A}$$

(1.10)

To consider transverse deformation, Poisson ratio υ can be applied,

$$\varepsilon_y = -\upsilon\varepsilon_x$$

(1.11)

The cross-section area consists of a width w and thickness t. If a wire with length L is on deformation with strain ε in the length direction, its width w and thickness t will change according to

$$L^* = L(L + \varepsilon) \tag{1.12}$$

$$w^* = w(1 - \upsilon\varepsilon) \tag{1.13}$$

$$t^* = t(1 - \upsilon\varepsilon) \tag{1.14}$$

If the area strain is the sum or the width and thickness strain, then relative area change is described by equation,

$$\frac{\Delta A}{A_0} = \frac{\Delta w}{w_0} + \frac{\Delta t}{t_0} \tag{1.15}$$

The definition of the Poisson ratio gives equation (1.16)

$$\frac{\Delta A}{A_0} = -2\upsilon\frac{\Delta L}{L_0} = -2\upsilon\varepsilon \tag{1.16}$$

Then equation (1.10) can be transformed as follows.

34

$$\frac{\Delta R}{R} = \frac{\Delta \rho}{\rho} + (1 + 2\upsilon)\varepsilon \qquad (1.17)$$

Fraction of electrical resistivity change is proportional to fraction of volume change,

$$\frac{\Delta \rho}{\rho} = m \frac{\Delta V}{V} \qquad (1.18)$$

where m is a material constant. Substituting equation (1.17) with equation (1.18), a well-known equation (1.19) can be obtained,

$$\frac{\Delta R}{R} = \varepsilon\{(1 + 2\upsilon) + m(1 - 2\upsilon)\} = K\varepsilon \qquad (1.19)$$

where K is a proportionality constant called a gage factor. This gauge factor has been used as a measure of the piezoresistance sensitivity.

In case of composites, piezoresistance can be affected by many factors such as the applied stress, filler morphology, filler spatial arrangements, filler volume fraction, matrix compressive modulus and tunneling distance. Filler morphology such as diameter of carbon fiber is important factor to the piezoresistance property. Shui *et al*. [76] studied the filler functionality with carbon fiber and carbon filaments. The carbon

35

filaments filled composites shows linear relation between resistivity change and applied strain, while carbon fiber filled one does not. They conclude this may be coming not from the change in separation between the fibers, but probably from the change in degree of straightness of the fibers. In addition, spatial arrangements of the fillers can influence the piezoresistance effects with increasing uniaxial stress or strain. Lu *et al.* [77] reported that there are two competing mechanism under compression in their graphite nanosheets (GNs) / PE composites. Up to a pressure, resistivity decreases slightly with increasing compression force. At low pressure, the interparticle separation decreases with increasing pressure, thereby resistivity decreases. However, beyond a critical point, resistivity increases because the reorientation of the GNs, and relative orientation of the anisotropic particles increases. Therefore piezoresistive effects strongly depend on the conductive network deformation, can be influenced by the filler morphology, filler spatial arrangement, and filler concentration.[78]

Young's modulus of polymer matrix is important for its piezoresistive behavior. Equation (1.20) describes the relation between Young's modulus and fractional resistance changes.

$$\frac{\Delta R}{R} = 12 \frac{K}{E} \frac{ld}{wt^3} F$$

(1.20)

where $\Delta R/R$ is the relative change in resistance and K is the gauge factor of the piezoresistor respectively, E is Young's modulus, l, w, t are the length, width, and thickness of the cantilever, d is the distance from the piezoresistor to the neutral axis, and F is the force applied at the apex of the cantilever. This equation (1.20) shows the relation between the gauge factor and Young's modulus of a material that determines the sensitivity of the cantilever sensor.[79]

Piezoresistance response of filler filled composites has been utilized to reveal the origin of non-universality of exponent t.[60, 80, 81] Grimaldi et al. [81] reported that universality breakdown may be due to the fluctuations in tunneling distances of RuO_2 filled thick-film resistors (TFRs). Piezoresistance coefficient Γ has been calculated and fitted using equation (1.21)

$$\Gamma \cong \Gamma_0 - B\ln(x - x_c)$$

(1.21)

where $\Gamma_0 = \dfrac{d\ln(R_0)}{d\varepsilon}$, $B = \dfrac{dt}{d\varepsilon}$

(1.22)

By using the equation (1.21) we can think about the influence of the applied strain on the universality of the critical exponent t. In general, a tensile strain increase the inter-

grain tunneling resistances leading to an overall enhancement of the sample resistance, so that piezoresistance coefficient must be positive. Therefore the value of B is important and they found the value of B becomes positive when the critical exponent is non-universal. Hence Grimaldi *et al*. concluded that the critical exponent *t* is affected by ε, giving evidence of a tunneling distance dependence of *t*.

2.7. Dielectric Electroactive Actuator (DEA)

An actuator is a device which transforms input energy to mechanical output energy. With this simple concept, electromagnetic actuators have been employed in various applications. However, there is a need for improved actuators in small–scale systems, such as micro robots and micro devices because conventional electromagnetic actuators are inferior in the efficiency at the small scale [82]. Therefore electroactive polymer (EAP) materials have been much interest because they are lightweight, high strain level, fast response speeds, low hysteresis and low cost [82-84]. These EAPs have important potential applications in transducer, sensor, and actuator technologies [85]. Out of EAPs, electrostrictive polymer actuators, also known as Dielctric Elastomer Actuators (DEA), have been spotlight because the material, dielectric elastomer, exhibits natural muscle-

like behavior and easy to process [86-89]. Therefore the actuating performances of DEAs have been assessed and continuously improved during the last few years [87-91].

In general, a capacitor consists of insulator or dielectric material and two electrodes. This capacitor structure is like a structure of the dielectric elastomer structure. The primary use of capacitor is the store charges or energy. This performance is also similar to the mechanism of DEA. Therefore a DEA can be considered as a compliant capacitor. DEAs consist of a dielectric elastomer film sandwiched between two compliant electrodes. A voltage difference is applied between the compliant electrodes, causing compression in thickness and stretching in area of the polymer film. DEA uses electrostatic force to provide the driving motion instead of using ionic effect. When a high electric field is applied to both electrodes of the actuator, electrostatic forces are generated between free charges on each compliant electrode. This generated electrostatic force by the high electric field results in expanding the electrodes in area as well as shrinking the elastomer in thickness. This stretching in area of the electrode is due to the repulsive force between like charges on the electrode whereas shrinking in thickness of the elastomer is due to the attractive force between opposite charges of mutual electrodes. This phenomenon is known as Maxwell stress or pressure [86, 92]. These two simultaneous modes of energy conversion are described in Figure 2.6.
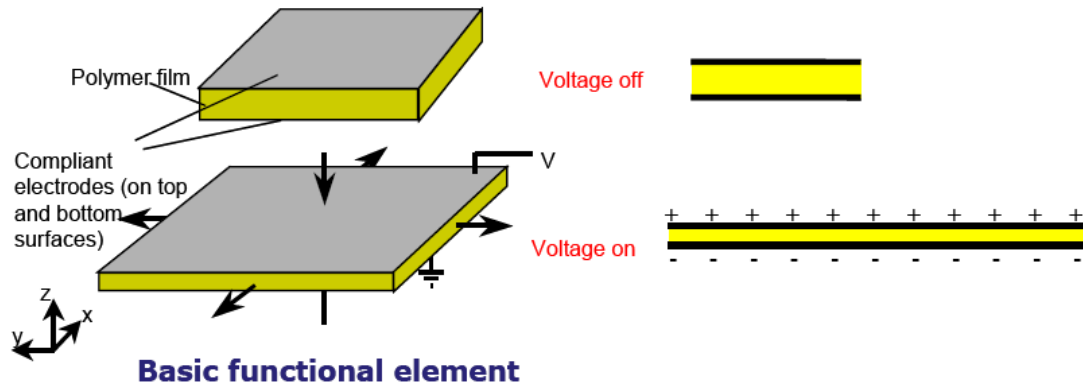
Figure 2.6. Principle of operation of DEAs [88].

Key factors of DEA are dielectric elastomer and compliant electrode. Commonly used dielectric elastomers for an actuator are silicones [82, 87, 90], and acrylic elastomers [91, 92]. These two elastomers are not crystalline but amorphous polymers. Polymer materials, which are amorphous, have their polymer chains randomly oriented. Dielectricity arises from the affinity that polar molecules align themselves with an external electric field. When high electric filed is applied to the dielectric polymer, polar segments or dipole segments of the polymer chains are aligned along the electric field direction. Therefore current does not flow through the dielectric material but are stored in dielectric elastomers. This is why dielectric material is useful for the capacitor and actuator materials. Silicones and acrylic elastomers, both dielectric elastomers, have shown the best performance as artificial muscle actuator materials. Experimental

testings in the area of dielectric elastomers have focused on two specific materials, namely CF 1921-86 a silicone from NuSil and VHB 4910 an acrylic manufactured by 3M. Actuated strains of up to 117% have been achieved with silicone elastomers and up to 215% for acrylic elastomers [89]. Actuation pressures of 8 MPa and energy densities of 3 J/cm^3 have been demonstrated with acrylic and silicone elastomers [89]. This coupled with their fast response speeds and potentially high efficiencies make them attractive materials for the DEA.

2.8. References

1. Martin, C.A., Sandler, J., Shaffer, M., Schwarz, M. K., Bauhofer, W.,Schulte, K., and Windle, A. H., *Formation of Percolating Networks in Multi-wall Carbon-Nanotube-Epoxy Composites.* Composite Sci. and Tech., 2004. **64**: p. 2309.

2. Sandler, J., Kirk, J., Kinloch, I., Shaffer, M., and Windle, A., *Ultra-Low Electrical Percolation Threshold in Carbon-Nanotube-Epoxy Composites.* Polymer, 2003. **44**: p. 5893.

3. Ruan, S.L., Gao, P., Yang, X. G., and Yu, T. X., *Toughening High Performance Ultrahigh Molecular Weight Polyethylene Using Multiwalled Carbon Nanotubes.* Polymer, 2003. **44**: p. 5643.

4. Ash, B.J., Stone, J., Rogers, D. F., Schadler, L. S., Siegel, R. W., Benicewicz, B. C., and Apple, T., *Investigation into the Thermal and Mechanical Behavior of PMMA/Alumina Nanocomposites.* Mat. Res. Soc. Symp. Proc., 2001. **661**: p. KK2.10.1.

5. Naganuma, T., and Kagawa, Y., *Effect of Pparticle Size on the Optically Transparent Nano Meter-Order Glass Particle-Dispersed Epoxy Matrix Composites.* Compos. Sci. Technol., 2002. **62**(9): p. 1187.

6. Yoon, P., Fornes, T., and Paul, D., *Thermal Expansion Behavior of Nylon 6 Nanocomposites.* Polymer, 2002. **43**: p. 6727.

7. Zhang, S., and Horrocks, A. R., *A Review of Flame Retardant Polypropylene Fibres.* Prog. Polym. Sci., 2003. **28**: p. 1517.

8. Li, X., Chang, W., Chao, Y. J., Wang, R., and Chang, M., *Nanoscale Structural and Mechanical Characterization of a Natural Nanocomposite Materials: the Shell of Red Abalone.* Nano Lett, 2004. **4**: p. 613.

9. Gangopadhyay, R., and De, A., *Conducting Polymer Nanocomposites: A Brief Overview.* Chem. Mater., 2000. **12**: p. 608.

10. Schmidt, G., and Malwitz, M. M., *Properties of Polymer-Nanoparticle Composites.* Curr. Opin. Colloid Interface Sci., 2003. **8**: p. 103.

11. Hou, H., Ge, J. J., Zeng, J., lI, Q., Reneker, D. H., Greiner, A., and Cheng, S. Z. D., *Electrospun Polyacrylonitile Nanofibers Containing a High Concentration of Well-Aligned Multiwall Carbon Nanotubes.* Chem. Mater., 2005. **17**: p. 967.

12. Dror, Y., Salalha, W., Khalfin, R. L., Cohen, Y., Yarin, A. L., and Zussman, E., *Carbon Nanotubes Embedded in Oriented Polymer Nanofibers by Electrospinning.* Langmuir, 2003. **19**: p. 7012.

13. Zhang, X., Liu, T., Sreekumar, T.V., Kumar, S., Hu, X., and Smith, K., *Gel Spinning of PVA/SWNT Composite Fiber.* Polymer, 2004. **45**: p. 8801.

14. Wang, Y., Cheng, R., Liang, L., and Wang, Y., *Study on the Preparation and Characterization of Ultra-High Molecular Weight Polyethylene–Carbon Nanotubes Composite Fiber.* Compos Sci Technol, 2005. **65**: p. 793.

15. Sreekumar, T.V., Liu, T., Min, G. B., Guo, H., Kumar, S., Hauge, R., and Smalley, R. E., *Polyacrylonitrile Single-Walled Carbon Nanotube Composite Fibers.* Adv. Mater., 2004. **16**(1): p. 58.

16. Munoz, E., Suh, D., Collins, S., Selvidge, M., Dalton, A. B., Kim, B. G., Razal, J. M., Ussery, G., Rinzler, A. G., Martinez, M. T., and Baughman, R. H., *Highly Conducting Carbon Nanotube/Polyethylene Composite Fibers.* Adv Mater, 2005. **17**: p. 1064.

17. Siochi, E.J., Working, D. C., Park, C., Lillehei, P. T., Rouse, J. H., Topping, C. C., Bhattacharyya, A., and Kumar, S., *Melt Processing of SWCNT-Polyimide Nanocomposite Fibers.* Composites: Part B, 2004. **35**: p. 439.

18. Ko, F., Gogotsi, Y., Ali, A., Naguib, N., Ye, H., Yang, G., Li, C., and Willis, P., *Electrospinning of Continuous Carbon Nanotube-Filled Nanofiber Yarns.* Adv. Mater., 2003. **15**(14): p. 1161.

19. Sen, R., Zhao, B., Perea, D., Itkis, M. E., Hu, H., Love, J., Bekyarova, E., and Haddon, R. C., *Preparation of Single-Walled Carbon Nanotube Reinforced Polystyrene and Polyurethane Nanofibers and Membranes by Electrospinning.* Nano Lett., 2004. **4**: p. 459.

20. Seoul, C., Kim, Y., and Baek, C., *Electrospinning of Poly(vinylidenefluoride)/Dimethylformamide Solutions with Carbon Nanotubes.* J Polym Sci, Part B: Polym Phys, 2003. **41**: p. 1572.

21. Pedicini, A., and Farris, R. J., *Thermally Induced Color Change in Electrospun Fiber Mats.* J Polym Sci, Part B: Polym Phys, 2004. **42**: p. 752.

22. Mack, J.J., Viculis, L. M., Ali, A., Luoh, R., Yang, G., Hahn, H. T., Ko, F. K., and Kaner, R. B., *Graphite Nanoplatelet Reinforcement of Electrospun Polyacrylonitrile Nanofibers.* Adv. Mater., 2005. **17**(1): p. 77.

23. Hong, J.H., Jeong, E. H., Lee, H. S., Baik, D. H., Seo, S. W., and Youk, J. H., *Electrospinning of Polyurethane/Organically Modified Montmorillonite Nanocomposites.* J Polym Sci, Part B: Polym Phys, 2005. **43**: p. 3171.

24. Ge, J.J., Hou, H., Li, Q., Graham, M. J., Greiner, A., Reneker, D. H., Harris, F. W., and Cheng, S. Z. D., *Assembly of Well-Aligned Multiwalled Carbon Nanotubes in Confined Polyacrylonitrile Environments: Electrospun Composites Nanofiber Sheets.* J. Am. Chem. Soc., 2004. **126**: p. 15754.

25. Gao, J., Yu, A., Itkis, M. E., Bekyarova, E., Zhao, B., Niyogi, S., and Haddon, R. C., *Large-Scale Fabrication of Aligned Single-Walled Carbon Nanotube Array and Hierarchial Single-Walled Carbon Nanotube Assembly.* J. Am. Chem. Soc., 2004. **126**: p. 16698.

26. Salalha, W., Dror, Y., Khalfin, R. L., Cohen, Y., Yarin, A. L., and Zussman, E., *Single-Walled Carbon Nanotubes Embedded in Oriented Polymeric Nanofibers by Electrospinning.* Langmuir, 2004. **20**: p. 9852.

27. Doshi, J., and Reneker, D., J Electrostatics, 1995. **35**: p. 151.

28. Huang, Z., Zhang, Y., Kotaki, M., and Ramakrishna, S., Compos Sci Technol, 2003. **63**: p. 2223.

29. Formhals, A., *Process and Apparatus for Preparing Artificial Threads.* U.S. Patent 1,975,504, 1934.

30. Taylor, G.I., Proc R Soc London, Ser A, 1969. **313**: p. 453.

31. Baumgarten, P.K., J. Colloid Interface Sci., 1971. **36**: p. 71.

32. Tsai PP, S.-G.H., Gibson P, *Different Electrostatic Methods for Making Electret Filters.* J Electrostatics, 2002. **54**: p. 333.

33. Xu, C.Y., Inai, R., Kotaki, M., and Ramakrishna, S., Biomaterials, 2004. **25**: p. 877.

34. Wang, X., Drew, C., Lee, S. H., Senecal, K. J., Kumar, J., and Samuelson, L.A., *Electrospun Nanofibrous Membranes for Highly Sensitive Optical Sensors.* Nano Lett, 2002. **2**: p. 1973.

35. Ma M, M.Y., Gupta M, Gleason KK, Rutledge GC, *Superhydrophobic Fabrics Produced by Electrospinning and Chemical Vapor Deposition.* Macromolecules, 2005. **38**: p. 9742.

36. Kim, C., and Yang, K. S., *Electrochmical Properties of Carbon Nanofiber Web as an Electrode for Supercapacitor Prepared by Electrospinning.* Appl. Phys. Lett, 2003. **83**: p. 1216.

37. Huang, J., *Carbon Black Filled Conducting Polymers and Polymer Blends.* Adv Polym Technol, 2002. **21**: p. 299.

38. Warren, B.E., *X-Ray Diffraction Study of Carbon Black.* J. Chem. Phys., 1934. **2**: p. 551.

39. Franklin, R.E., *Crystallite Growth in Graphitizing and Non-Graphitizing Carbons.* Proc. Royal. Soc., 1950. **A209**: p. 196.

40. Sweitzer, C.W., and Heller, G. L., *The Formation of Carbon Black in Hydrocarbon Flames.* Rubber World, 1956. **134**: p. 855.

41. Fitzer, E., and Manocha, L. M., *Carbon Reinforcement and Carbon/Carbon Composites.* 1998: p. 342.

42. Donnet, J., and Bansal, R. C., *Carbon Black: Science and Technology.* 1993.

43. Ergun, S., *Structure of Carbon.* Carbon, 1968. **6**: p. 141.

44. Donnet, J., *Fifty Years of Reserch and Progress on Carbon Black.* Carbon, 1994. **32**: p. 1305.

45. Medalia, A.I., *Electrical Conduction in Carbon Black Composites.* Rubber Chem. Tech., 1986. **59**: p. 432.

46. Balberg, I., *Tunneling and Nonuniversal Conductivity in Composite materials.* Phys. Rev. Lett., 1987. **59**(12): p. 1305.

47.   Balberg, I., *A Comprehensive Picture of the Electrical Pphenomena in Ccarbon Black–Polymer Composites.* Carbon, 2002. **40**: p. 139.

48.   Carmona, F., *Conducting Filled Polymers.* Physica A, 1989. **157**: p. 461.

49.   Polley, H., and Boonstra, B., Rubber Chem. Tech., 1957. **30**: p. 170.

50.   Sichel, E.K., Gittleman, J. I., Sheng, P., and Princeton, N. J., *Electrical Properties of Carbon-Polymer Composites.* J. Electron. Mater., 1982. **11**(4): p. 699.

51.   Abeles B., P.H.L., Gittleman J. I., *Percolation Conductivity in W-Al$_2$O$_3$ Granular Metal Films.* Phys. Rev. Lett., 1975. **35**: p. 247.

52.   Kirkpatrick, S., *Percolation and Conduction.* Rev. Mod. Phys., 1973. **45**: p. 574.

53.   Sheng, P., Sichel, E. K., and Gittleman, J. I., Phys. Rev. B., 1978. **18**: p. 5712.

54.   Sheng, P., Sichel, E. K., and Gittleman, J. I., *Fluctuation-Induced Tunneling Conduction in Carbon-Polyvinylchloride Composites.* Phys. Rev. Lett., 1978. **40**: p. 1197.

55.   Sichel, E.K., Gittleman, J. I. and Sheng, P., *Transport Properties of The Composite Material Carbon-Poly(Vinyl Chloride).* Phys. Rev. B, 1978. **18**: p. 5712.

56.   Mantese JV, C.W., Webb WW, *Two-Component Model for the Resistivity and Noise of Tunnelin g Metal-Insulator Composites.* Phys Rev B, 1986. **33**: p. 7897.

57. Heaney, M.B., *Measurement abd Interpretation of Nonuniversal Critical Exponents in Disordered Conductor-Insulator Composites.* Phys. Rev. B, 1995. **52**: p. 12477.

58. Rubin, Z., Sunshine, S. A., Heaney, M. B., and Balberg, I., Phys. Rev. B, 1999. **59**: p. 12196.

59. Balberg, I., and Bozowski, S., Solid State Commun., 1982. **44**(4): p. 551.

60. Grimaldi, C., Maeder, T., Ryser, P., and Strassler, S., *Piezoresistivity and Conductance Anisotropy of Tunneling-Percolating Systems.* Phys. Rev. B, 2003. **67**: p. 014205.

61. Sherman, R.D., Middleman, L. M., and Jacobs, S. M., *Electron Transport Processes in Conductor-Filled Polymers.* Polym. Eng. Sci., 1983. **23**(1): p. 36.

62. Schiff, L.I., *Quantum Mechanics, 3rd ed.*, Neyork, McGraw-Hill Book, 1968.

63. Sichel, E.K., *Carbon Black-Polymer Composites.* 1982.

64. Tang, H., Chen, X., Tang, A., and Luo, Y., *Studies on the Electrical Conductivity of Carbon Black Filled Polymers.* J. Appl. Polym. Sci., 1996. **59**: p. 383.

65. Bueche, F.J., J. Appl. Phys., 1973. **44**: p. 532.

66. Toker, D., Azulay, D., Shimoni, N.,Balberg, I., and Millo, O., Phys. Rev. B, 2003. **68**: p. 041403.

67.   Zallen, R., *The Physics of Amorphous Solids.*, New York, Jhon Wiley & Sons, 1983

68.   Bueche, F.J., *Electrical resistivity of conducting particles in an insulating matrix.* J. Appl. Phys., 1972. **43**: p. 4837.

69.   McLachlan, D.S., M.B., and Newnham, R. E., *Electrical Resistivity of Composites.* J. Am. Ceram. Soc., 1990. **73**: p. 2187.

70.   McLachlan, D.S., J. Appl. Phys., 1990. **68**: p. 195.

71.   Clingerman, M.L., King, J. A., Schulz, K. H., Meyers, J. D., J. Appl. Polym. Sci., 2002. **83**: p. 1341.

72.   Blaszkiewicz, M., McLachlan, D. S., and Newnham, R. E., Polym. Eng. Sci., 1992. **32**: p. 421.

73.   Lei, H., Pitt, W. G., McGrath, L. K., Ho, C. K., *Resistivity Measurements of Carbon - Polymer Composites in Chemical Sensors: Impact of Carbon Concentration and Geometry.* Sensors and Actuators B, 2004. **101**(122).

74.   Yi, X., Wu, G., and Pan, Y., *Properties and Applications of Filled Conductive Polymer Composites.* Poly. Int., 1997. **44**: p. 117.

75. Marquez, A., Uribe, J., Cruz, R., *Conductivity Variation Induced by Solvent Swelling of an Elastomer-Carbon Black-Graphite Composite.* J. Appl. Polm. Sci., 1997. **66**: p. 2221.

76. Shui, X., and Chung, D. D. L., *A Piezoresistive Carbon Filament Polymer-Matrix Composite Strain Sensor.* Smart Mater. Struct., 1996. **5**: p. 243.

77. Lu J, C.X., Lu W, Chen G, *The Piezoresistive Behaviors of Polyethylene/Foliated Graphite Nanocomposites.* Eur Polym J, 2006. **42**: p. 1015.

78. Lu, J., Weng, W., Chen, X., Wu, D., and Chen, G., *Piezoresistive Materials from Directed Shear-Induced Assembly of Graphite Nanosheets in Polyethylene.* Adv. Funct. Mater., 2005. **15**: p. 1358.

79. Gammelgaard, L., Rasmussen, P. A., Calleja, M., Vettiger, P., and Boisen, A., *Microfabricated Photoplastic Cantilever with Integrated Photoplastic/Carbon Based Piezoresistive Strain Sensor.* Appl. Phys. Lett, 2006. **88**: p. 113508.

80. Vionnet-Menot, G., C., Maeder, T., Ryser, P., and Strassler, S., *Study of Electrical Properties of Piezoresistive Pastes and Determination of the Electrical Transport.* J. Eur. Ceram. Soc., 2005. **25**: p. 2129.

81. Grimaldi, C., Maeder, T., Ryser, P., and Strassler, S., *Critical Behavior of the Piezoresistive Response in RuO₂-Glass Composites*. J. Phys. D: Appl. Phys., 2003. **36**: p. 1341.

82. Perline, R., Kornbluh, R., Joseph, J., Heydt, R., Pei, Q., and Chiba, S, *High-Field Deformation of Elastimeric Dielectrics for Actuators*. Mat. Sci Eng. C, 2000. **11**: p. 89.

83. Zhang, Q.M., Li, H., Poh, M. Xia, F., Cheng, Z. Y., Xu, H., Huang, C., *An All-Organic Composite Actuator Material With a High Dielectric Constant*. Nature, 2002. **419**(19): p. 284.

84. Liu, C., Bar-Cohen, Y. and Leary, S., *Electro-Statically Stricted Polymers (ESSP)*. SPIE, 1999. **3669**: p. 186.

85. Cheng, Z.Y., Xu, H. S., Su, J., Zhang, Q. M., Wang, P. C., andd MacDiarmid, A. G., *High Performance of All-Polymer Electrostrictive Systems*. SPIE, 1999. **3669**: p. 140.

86. Perline, R.E., Kornbluh, R. D., and Joseph, J. P., *Electrostriction of Polymer Dielectrics with Compliant ELectrodes as a Means of Actuation*. Sensors and Actuators A, 1998. **64**: p. 77.

87. Carpi, F., Migliore, A., Serra, G., and Rossi, D. D., *Helical Dielectric Elastomer Actuators*. Smart Mater. Struct., 2005. **14**: p. 1210.

88. Perline, R., Kornbluh, Pei, Q., Stanford, S., Oh, Seajin, Eckerle, J., Full, R., Rosenthal, M., Meijer, K., *Dielectric Elastomer Artificial Muscle Actuators: Toward Biomimetic Motion*. Proc. SPIE, 2002. **4695**: p. 126.

89. Perline, R., Kornbluh, R. D., Pei, Qibing, and Joseph, J., *High-Speed Electrically Actuated Elastomers with Strain Greater Than 100%*. Science, 2000. **287**: p. 836.

90. Lacour, S.P., Prahlad, H., Perline, R., Wagner, S., *Mechatronic System of Dielectric Elastomer Actuators Addressed by Thin Film Photoconductors on Plastic*. Sensors and Actuators A, 2004. **111**: p. 288.

91. Carpi, F., Chiarelli, P., Mazzoldi, A., and Rossi, D. D., *Electromechanical Characterisation of Dielectric Elastomer Planar Actuators: Comparative Evaluation of Different Electrode Materials and Different Counterloads*. Sensors and Actuators A, 2003. **107**: p. 85.

92. Kofod, G., Sommer-Larsen, P., Kornbluh, R., and Pelrine, R., *Actuation Response of Polyacrylate Dielectric Elastomers*. J. Intell. Mater. Syst. Struct., 2003. **14**: p. 787.

CHAPTER 3.

PERCOLATION THRESHOLD OF CARBON BLACK FILLED

ELECTROSPUN NANOCOMPOSITE FIBER: SIMULATION OF

PERCOLATION BEHAVIOR

3.1. Abstract

The percolation behavior of the nanocomposite fiber filled with carbon black was simulated. We demonstrated that the percolation threshold of the nanocomposite fiber filled with carbon black could be obtained at carbon black volume fraction as low as 9.3 vol% theoretically. Moreover, as particle size and tunneling distance increases, percolation threshold increases.

Key words: Carbon Black, Nanocomposite fiber, Percolation threshold, HK algorithm

3.2. Introduction

Normally insulating polymers with good mechanical properties such as polyurethane, and rubber can be made conductive by the addition of nano to micron

sized carbonaceous fillers such as carbon black, carbon nanotubes, and graphite or metallic particles such as colloidal silver or gold. By making these polymers conductive new classes of nanostructured functional materials can be created for potential use in a variety of applications, including sensors and compliant electrodes. In this paper we simulate with percolation theory the onset of conductivity as a function of particle size, and investigate experimentally the use of carbon nanoparticles as a means of producing conductive nano/polymer nanocomposites fiberwebs using electro spinning techniques.

The electrical conduction in conductive filler loaded composite is mainly determined by three mechanisms, quantum tunneling between isolated conductive particles [1-5], percolation in a continuous conductive network where the particle make direct physical contact [5-7], and coexistence of tunneling and percolation [8]. In the first case, when the distance between particles is sufficiently small and an electric field is applied, the electrons can tunnel from one particle to another through the potential barrier of the surrounding polymer [9, 10]. According to Balberg [11], the tunneling probability decays exponentially with the distance between particles. This distance is called tunneling distance. Sherman [9] reported that electrons can tunnel quantum mechanically between conductive elements when proximity between two conductive particles is small in polymer matrix (≤ 100 Å).   Medalla [2] also reported that tunneling

distance may be of the order of 15-100 Å in carbon black filled polymer composite. For conduction to occur throughout the nanocomposite a network of particles sufficiently close together needs to be formed before conduction occurs. In the second case, as the amount of the conductive fillers in the composite increases, the particles of the fillers begin to make direct contact to each other, and continuous conduction path can be formed through the composite. Both cases can be investigated using percolation theory to predict the transition from the insulating state to the conductive state as a function of the amount of conductive materials in the nanocomposite. The last case, coexistence of tunneling and percolation, is demonstrated by the change of electrical resistivity of polymer composite when the temperature changes [3], or on application of strain [10, 12]. Examples of such systems are provided by various carbon-black–polymer composites [8], and thick-film resistors [12] made of metal-oxide conductive grains randomly dispersed in a glassy matrix.

Percolation theory has been used to investigate metal-insulator composites [5, 13] where above a threshold the continuous network of contacting particles dominates and below threshold thermally assisted charge tunneling can results in residual conductivity in the nominally insulating state [5]. Similarly, carbon black particles dispersed into polymers can be investigated by percolation theory [8, 11] because the percolation

theory is a probability theory dealing with properties of random media or a disordered system [14].

In this research, the percolation behavior of nanocomposite fiber filled with CB has been simulated. To generate the necessary CB particle dispersed system, Monte Carlo method was used and to analyze the percolation path of CB particles in the matrix, Hoshen and Kopelman algorithm[15] was used. The main objective of performing the computer simulations of the carbon black filled nanofiber system was to explore the relationship between particle content and electrical conductivity of the composite fiberweb. It is important to note that for the purpose of simulation, fiber behavior is assumed to represent fiberweb behavior. The assumption, therefore, precludes any influence of fiberweb structure on its electrical behavior. This may not be overly simplified in light of the fiber dimension (diameter ~1μm) relative to fiberweb thickness (>50μm). In addition, two mechanisms of conduction, inter-particle tunneling and classical percolation are assumed to be at work to generate electrical conductivity within the nanocomposite fiber.

3.3. Background

In general, to model percolation systems, the system is described as a lattice where each node consists of randomly distributed conducting and isolating sites. When a continuous path from one boundary of the medium to another boundary can be formed by connecting adjacent conductive lattice sites the percolation threshold is exceeded and a spanning cluster is said to be formed. In general, when the lattice is large it can be computationally hard to determine the number and size of clusters and to distinguish if a specific site belongs to a spanning cluster. Since, in general, the distribution of conductive sites is considered to be random, the problem is also statistical in nature, which increases the computational burden by requiring multiple computations to be performed.

The Hoshen and Kopelman algorithm (HK) [15] is a relatively computationally efficient algorithm that enables one to assign each conductive lattice point a label to determine if it belongs to a specific cluster. Then by examining the labels at the boundaries of the lattice one can determine if a spanning cluster has been formed. Recently the HK algorithm has been extended to allow Monte Carlo simulations of large lattice to determine information not only on the cluster size but also on the structure of the clusters [16-18]. Since the percolation threshold can be dependent on the

nature of the lattice both super network [19], and cubic lattices [19] were of interest in this study. These lattices are thought to be the most representative of our physical system consisting of nanoparticles in polymer since they generally represent systems with close packed spheres well.

Monte Carlo method has been widely used for simulation in many diverse fields including filler loaded composite [20-22]. It is based on the deliberate use of random number or random sampling from a certain distribution of the sample. A large number of trials in the simulation provide the average values of macroscopic quantities which is close to the experimental values. In this view Monte-Carlo simulation can be applied to the percolation system.

In the percolation system a random number r ($0 < r < 1$) is generated with uniform distribution into each site in the matrix. The generated number is then compared to given probability p which represents volume fraction of the filler (also occupation probability). If the generated number r is smaller than given probability p, that site is considered as occupied, if not, that site is left unoccupied. Since each appearance of an occupied site has probability p, each appearance of an empty site has probability ($1-p$), the whole configuration appears with probability [23]

$$p^m (1-p)^{L^d - m} \qquad (3.1)$$

where $d = 2$ is the dimension, $m = \Sigma n(i,j)$ is the total number of occupied sites, and L is

the size of the system (L×L system).

This procedure is repeated for the given number of trial. Percolation probability

(*PP*) and volume fraction of occupied sites are calculated every time a trial is completed.

Percolation probability (*PP*) is the probability that any arbitrarily selected site belongs

to the spanning cluster. *PP* is given by equation below [23]

$$PP = \frac{\text{number of sites in the infnite cluster}}{\text{total number of sites}} \qquad (3.2)$$

Clearly for $p < p_c$, the percolation probability $PP = 0$ because there exists no infinite

cluster. For $p > p_c$, the quantity *PP* becomes positive and approaches 1 as p goes to 1.

The quantities *PP* and p are related by equation below

$$PP + \sum n_s s = p \qquad (3.3)$$

Thus percolation threshold can be determined by using this equation (3.3) because there is a significant increase of percolation probability, *PP,* on the percolation threshold. The average of percolation probability *PP* can be estimated by Monte Carlo simulation. That is given by

$$\langle PP \rangle = \frac{1}{N} \sum_{j=1}^{N} PP_j \tag{3.4}$$

where N is the number of trial, and *<PP>* is the average of percolation probability

The normalized percolation probability (NPP) can be given by

$$NPP = \frac{the\ average\ of\ percolation\ probability}{given\ occupation\ probability} = \frac{<PP>}{p} \tag{3.5}$$

This normalized percolation probability makes percolation probability data more sensitive to the percolation threshold, and makes percolation threshold more easily identifiable. In this research percolation threshold is defined as the volume fraction of conductive filler when the normalized percolation probability is rapidly increasing.

3.4. Experimental

The simulation used in this work was intended to determine the percolation threshold of nanocomposite fibers produced using electrospinning. The simulation was also meant to elucidate factors influencing the electrical resistance of the fiber-webs. To this end, the HK algorithm was implemented using Matlab ver. 7.0 with typical lattice sizes determined by the particle size of the conducting filler.

In implementing the model for simulation it is assumed that the particles are spherical and that the electrical conduction can take place due to quantum tunneling between CB particles. In other words it is assumed that for a characteristic distance between particles (less than or equal to the tunneling distance) the conduction would occur giving an effective particle size larger than the physical size of the particles. Since the percolation threshold of nanocomposite fibers can be dependent on the nature of the lattice, two different networks were examined; simple cubic lattice with six nearest neighbors and super-network with twenty six nearest neighbors [19], see Figure 3.1 (a) and (b). The assumption of 6 neighboring sites for cubic sites is obvious, however, the assumption of 26 neighboring sites was included to simply model a super conductive network Additionally, simplified assumptions were necessary to simulate a fiber shape and its length to make the calculation computationally viable. Since nanofiber by

electrospinning produces long thin fibers with diameters ranging from 30 nm to more than a micrometer and lengths of up to several microns [24], it was not practical to simulate the entire fiber. Instead fiber length equal to 100 times the particle diameter were populated in the simulation. Once computed, the fiber was assumed to be representative of the entire nanofiber population.

The computer program using Matlab to determine the percolation threshold used is described by the flowchart presented in Figure 3.2. Where, percolation probability, PP, is equal to the number of sites in the spanning cluster divided by the total number of sites. Percolation probability (PP) is normalized by dividing it by occupation probability and has been designated as NPP. Using both measures, the percolation threshold can be found. Using the normalized percolation probability as a parameter the phase transition of the composite from insulator to conductor becomes more pronounced.

(a)   (b)
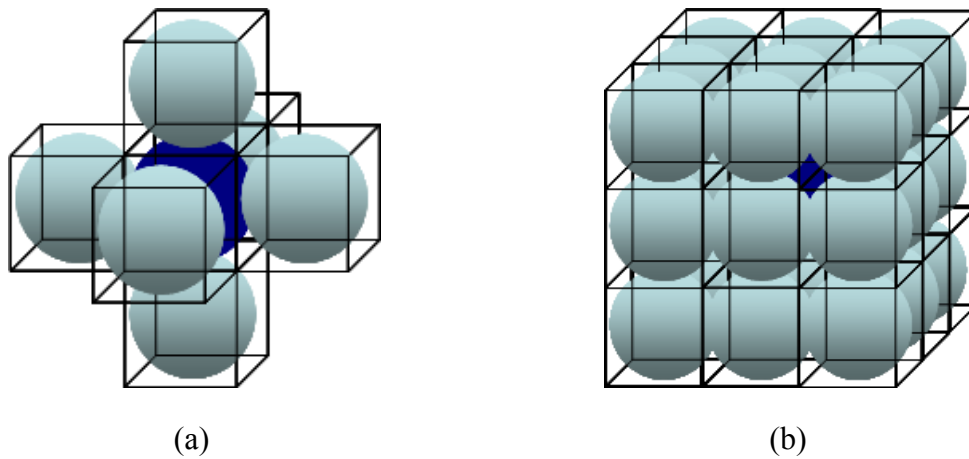
Figure 3.1. Visualizations of lattices used in the simulation: (a) cubic network, (b) super network.
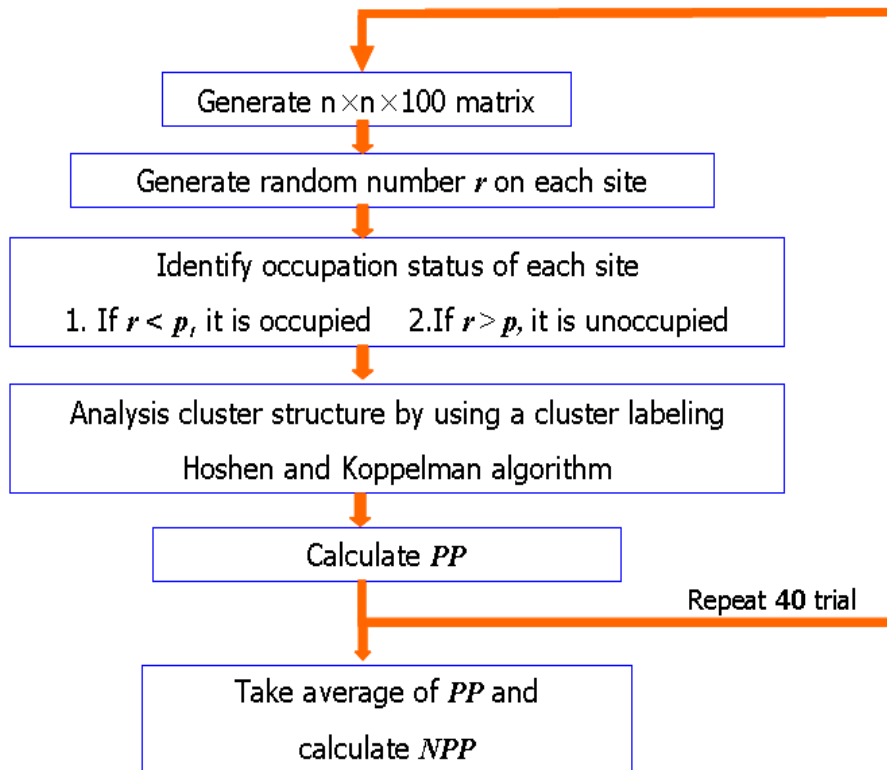
Figure 3.2. Schematic of percolation simulation procedure.

In performing the simulation, different values of the CB volume fraction (f) were used for determining the percolation threshold. Other important parameters in the simulation were particle size and tunneling distance. The range of diameter of CB particles are assumed to be 20-40 nm. The values of tunneling distance are assumed to be 2,6, and 10 nm. For the cubic network of 6 neighbors the volume fractions were varied from 20 to 60 vol%. For the super network of 26 neighbors, the volume fractions were varied from 5 to 40 vol% of CB. The parameters of the simulation in terms of the particle sizes and tunneling distance are summarized in Tables 3.1 and 3.2. Number of sites per layer represents number of sites generated in one layer. Number of overall sites stands for number of sites per layer times 100.

Table 3.1. Assumed parameter values to elucidate effect of particle size.

Sample No.	Diameter of Carbon Bblack Particle (nm)	Tunneling Distance (nm)	Effective diameter (nm)	Number of Sites per Layer	Number of Overall Sites
1-1	20	5	22.5	729	72,900
1-2	25	5	27.5	484	48,400
1-3	30	5	32.5	324	32,400
1-4	35	5	37.5	256	25,600
1-5	40	5	42.5	196	19,600

Table 3.2. Assumed parameter values to elucidate effect of tunneling distance.

Sample No.	Diameter of Carbon Black Particle (nm)	Tunneling Distance (nm)	Effective Diameter (nm)	Number of Sites per Layer	Number of Overall Sites
2-1	20	2	21	841	84,100
2-2	20	6	23	676	67,600
2-4	20	10	25	576	57,600

3.5. Results and Discussion

The normalized percolation probability values as a function of particle concentration for various particle sizes are plotted in Figure 3.3 (a) and (b) for cubic and super network respectively. Normalized Percolation probability represents the probability that any site belongs to a infinite cluster in the network matrix. In this context, percolation behavior can be represented by the NPP since it depends on the volume fraction of any filler material and percolation behavior is generally based on the formation of the percolation path in the medium. It can be observed that as the particle size increased, the percolation threshold as a function of volume fraction increased in both lattice types. Percolation thresholds is in the range of 33.3 to 36. 2 (vol% of CB) for the cubic lattice type. For the super network lattice type the percolation threshold range from 17.8 to 21.3 (vol% of CB). Both Figure 3.3 (a) and (b) show that the plot is not only shifting to higher volume concentration of carbon black, but also percolation threshold is

66

increased to higher volume concentration of carbon black as the particle size of the

carbon black increases. Similar observations were reported by Carcia et al. [25] for

metallic oxide based thick film resistors. For the super network type, a given site having

26 neighboring sites has greater probability to be in contact (physical or tunneling) with

neighborhood sites than the cubic type. This obviously resulted in lower percolation

threshold than the cubic type.

(a)   (b)
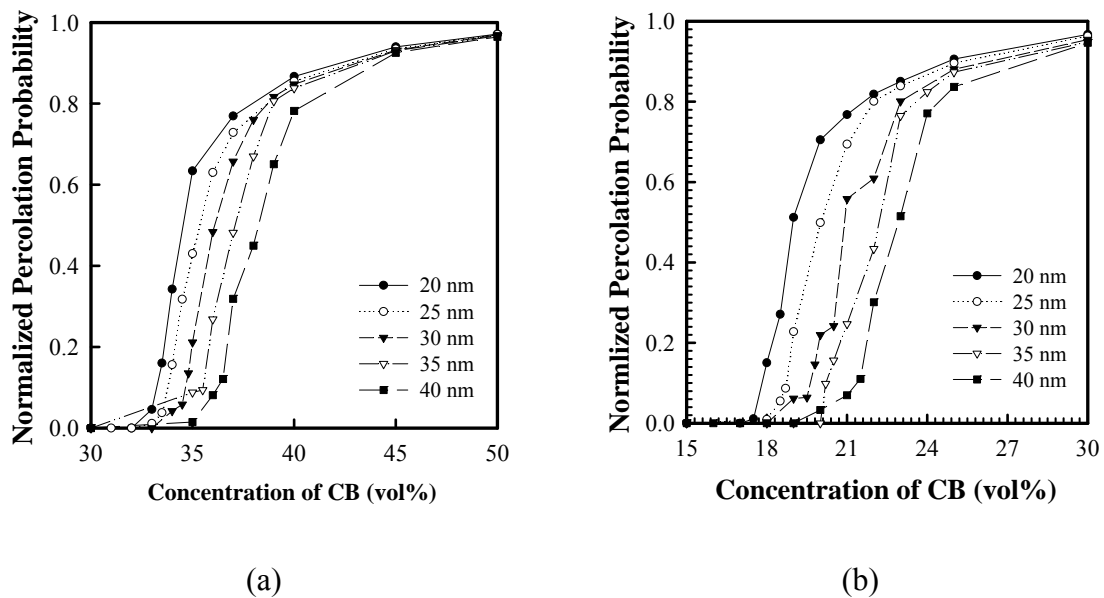
Figure 3.3. The influence of the particle size on the percolation behavior of electrospun

fiber: (a) cubic network, and (b) super network.

The effect of tunneling distance on percolation behavior of electrospun nanocomposite fiber is presented in Figures 3.4 (a) and (b). The effect of tunneling distance on the percolation behavior was studied with 3 different tunneling distances: 2, 6, 10 nm. Figure 3.4 shows that the percolation thresholds were moved higher location of the volume concentration. This result is similar to that discussed for particle size. However the effects of the tunneling distance are much lower than the particle sizes.

(a)   (b)
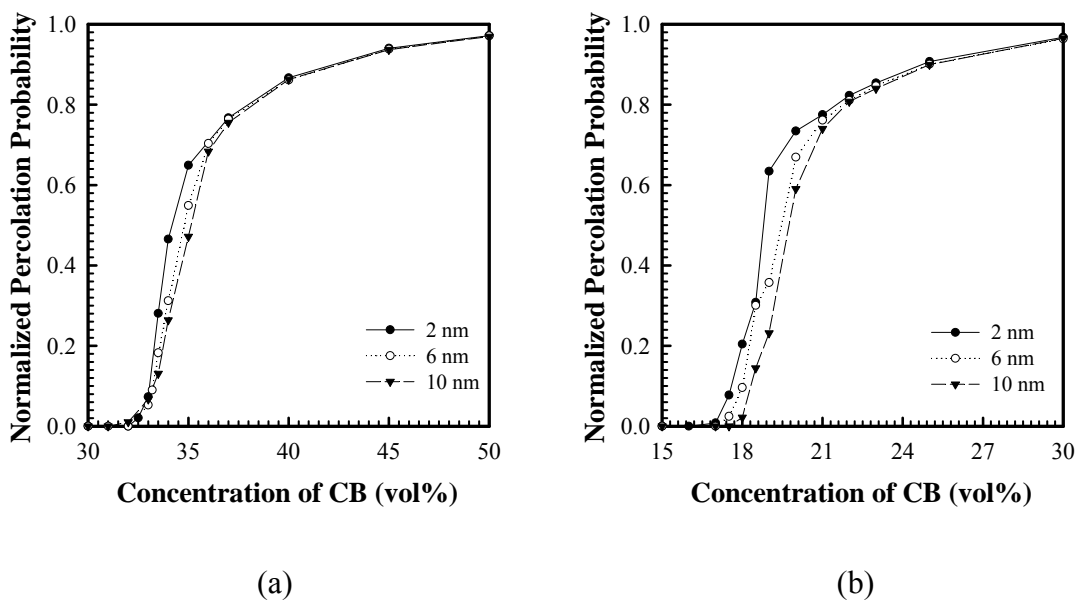
Figure 3.4. The influence of the tunneling distance on the percolation behavior of electrospun fiber: (a) cubic network, and (b) super network.

In terms of lattice choice, the super network lattice with a greater number of nearest neighbors exhibited a lower percolation threshold than cubic lattice. However, percolation threshold for various CB composites including PU/CB composites determined experimentally and reported in the literature is in the range of 2-12 vol% [26-28]. Using the cubic and super network lattices the simulation consistently overestimated the volume fraction. This can be attributed to the assumptions of uniform particle size and effective particle volume being equal to the lattice cell volume. In order to consider the actual particle shape (spherical) and its volume, the ratio of sphere volume to the cubic lattice cell volume equals 0.523, should be used as a correction factor. When the results are adjusted by this ratio, the percolation threshold of cubic lattice became 17.3 vol% and of super network became 9.3 vol%. This result is comparable to those observed experimentally in literatures.

3.6. Conclusions

The percolation behavior of the nanocomposite fiber filled with carbon black was simulated. Monte Carlo simulation method and HK algorithm was successfully employed to demonstrate and analysis the random particle dispersion in electrospun fiber matrix. In order to model the description of the continuous network of the carbon

black in nanocomposite fiber, two types of lattices were employed: cubic type and super network type. As expected, the super network type shows lower percolation threshold than the square type due to higher probability to contact neighborhood carbon particles. We demonstrated that the percolation threshold of the nanocomposite fiber filled with carbon black could be obtained at carbon black volume fraction as low as 9.3 vol%. Moreover, as particle size and tunneling distance increases, percolation threshold increases.

3.7. References

1. Sichel, E.K., Gittleman, J. I. and Sheng, P., *Transport Properties of The Composite Material Carbon-Poly(Vinyl Chloride)*. Phys. Rev. B, 1978. **18**: p. 5712.

2. Medalia, A.I., *Electrical Conduction in Carbon Black Composites*. Rubber Chem. Tech., 1986. **59**: p. 432.

3. Sheng, P., Sichel, E. K., and Gittleman, J. I., *Fluctuation-Induced Tunneling Conduction in Carbon-Polyvinylchloride Composites*. Phys. Rev. Lett., 1978. **40**: p. 1197.

4. Tang, H., Chen, X., Tang, A., and Luo, Y., *Studies on the Electrical Conductivity of Carbon Black Filled Polymers.* J. App. Polm. Sci., 1996. **59**: p. 383.

5. Abeles B., P.H.L., Gittleman J. I., *Percolation Conductivity in W-Al$_2$O$_3$ Granular Metal Films.* Phys. Rev. Lett., 1975. **35**: p. 247.

6. Kirkpatrick, S., *Percolation and Conduction.* Rev. Mod. Phys., 1973. **45**: p. 574.

7. Ehrburger-Dolle, F., Lahaye, J., and Misono, S., *Percolation in Carbon Black Powders.* Carbon, 1994. **32**(7): p. 1363.

8. Balberg, I., *A Comprehensive Picture of the Electrical Phenomena in Carbon Black–Polymer Composites.* Carbon, 2002. **40**: p. 139.

9. Sherman, R.D., Middleman, L. M., and Jacobs, S. M., *Electron Transport Processes in Conductor-Filled Polymers.* Polym. Eng. Sci., 1983. **23**(1): p. 36.

10. Grimaldi, C., Maeder, T., Ryser, P., and Strassler, S., *Piezoresistivity and Conductance Anisotropy of Tunneling-Percolating Systems.* Phys. Rev. B, 2003. **67**: p. 014205.

11. Balberg, I., *Tunneling and Nonuniversal Conductivity in Composite materials.* Phys. Rev. Lett., 1987. **59**(12): p. 1305.

12. Vionnet-Menot, G., C., Maeder, T., Ryser, P., and Strassler, S., *Study of Electrical Properties of Piezoresistive Pastes and Determination of the Electrical Transport.* J. Eur. Ceram. Soc., 2005. **25**: p. 2129.

13. Mantese JV, C.W., Webb WW, *Two-Component Model for the Resistivity and Noise of Tunnelin g Metal-Insulator Composites.* Phys Rev B, 1986. **33**: p. 7897.

14. Stauffer, D., *Introduction of Percolation Theory.*, London, Taylor & Francis, 1985.

15. J. Hoshen, a.R.K., Phys. Rev. B, 1976. **14**: p. 3438.

16. J. Hoshen, a.M.W.B., and K. S. Miner, Phys. Rev. B, 1997. **56**(1455).

17. A. Al-Futisi, a.T.W.P., Physica A, 2003. **321**: p. 665.

18. Yin, W.G., and Tao, R., *Rapid Algorithm for Identifying Backbones in the Two-Dimensional Percolation Model.* Int. J. Mod Phys C, 2003. **14**(10): p. 1427.

19. Wycisk, R., Pozniak, R., Pasternak, A, *Conductive Polymer Materials with Low Filler Content.* J Electrostatics, 2002. **56**: p. 55.

20. Pike, G.E., and Seager, C. H., Phys. Rev. B, 1974. **10**: p. 1421.

21. Heyes, D.M., J. Phys. Condens. Matter., 1990. **2**: p. 2241.

22. Li, P., and Strieder, J., J. Phys. C Solid State Phys., 1982. **15**: p. 6591.

23. Gould, H., Tobochink, J., and Christian, W., *An Introduction to Computer Simulation Methods, 3rd ed.* 2001.

24. Subbiah, T., Bhat, G. S., Tock, R. W., Parameswaran, and Ramkumar, S. S., *Electrospinning of Nanofibers.* J. Appl. Polym. Sci., 2005. **96**: p. 557.

25. Carcia, P.F., Ferretti, A., and Suna, A., *Particle Size Effects in Thick Film Resistors.* J. Appl. Phys., 1982. **53**: p. 5282.

26. Xiong C, Z.Z., Xu W, Hu H, Zhang Y, Dong L, *Polyurethane/Carbon Black Composites with High Positive Temperature Coefficient and Low Critical Tansformation Temperature.* Carbon, 2005. **43**: p. 1778.

27. Heiser JA, K.J., Konell JP, Sutter LL., *Electrical Conductivity of Carbon Filled Nylon 6,6.* Adv. Polym. Tech., 2004. **23**(2): p. 135.

28. Flandin, L., Chang, A., Nazarenko, S., Hiltner, A., and Baer, E., *Effect of Strain on the Properties of an Ethylene–Octene Elastomer with Conductive Carbon Fillers.* J. Appl. Polym. Sci., 2000. **76**: p. 894.

CHAPTER 4.

ELECTRICAL AND MECHANICAL PROPERTIES OF CARBON BLACK FILLED ELECTROSPUN NANOCOMPOSITE FIBERWEBS

4.1. ABSTRACT

The development of flexible and compliant conductive polymer composites with "textile" like characteristics remains an important endeavor in light of the recent activity in polymer/textile based electronics and the need for compliant electrodes for electroactive polymer actuators. In the present work, carbon black (CB) was dispersed in a polymer solution to form electrospun fiberwebs consisting mainly of nanofibers. The effect of filler content on fiberweb morphology, mechanical behavior, electrical conductivity, and thermal resistance has been examined. The electrical conductivity percolation threshold of the fiberweb structure is found to be around 4.6 vol%. Scanning electron micrographs of the fiberwebs reveal significant influence of CB content on fiber formation as well as the bond structure of the fiberweb which influences the mechanical properties of the web.

74

Key words: Electrospinning, Carbon black, Conductive fiberweb

4.2. Introdution

Compared to single phase materials the use of composite materials allows additional degrees of design freedom with which to tailor the physical properties of the composite for specific applications. Electrically conductive polymer matrix composites have attracted a great deal of interest because of their unique multifunctional properties such as the ability to combine elasticity with conductivity. Compared to metals they also are lighter weight and can potentially be easier to process. Specifically, normally insulating polymers with good mechanical properties such as polyurethane, and polyethylene can be made conductive by the addition of nano to micron sized conductive fillers such as graphitic particles, carbon black (CB), carbon nanotubes (CNT), or metallic particles such as colloidal silver or gold. Carbonaceous fillers have been routinely added to many polymers for various physical property enhancements including improving electrical conductivity for electrostatic discharge protection and to provide electromagnetic interference shielding, as wells as improving the thermal resistance or improvement of mechanical properties such as yield strength [1-4].

Conductive polymer composites are typically investigated in film form to elucidate their bulk behavior. However, polymers in thin film form can have limited flexibility or can be fragile mechanically. As a way to improve the mechanical characteristics while maintaining desired electrical conductivity the use of fiberwebs can be desirable since the fiber structure can provide flexibility to otherwise stiff materials, and the fiber network can provide structural strength.

Conductive fibers can be produced using a number of techniques. These include spinning of intrinsically conductive polymers [5] and incorporating conducting fillers in an insulating polymer matrix to form fibers [6, 7]. Spinning of intrinsically conducting polymers, however, present many problems including low solubility of the polymer. The relatively low conductivity of conductive polymers can also be limiting. On the other hand, significant increase in fiber conductivity can be achieved by incorporating conductive particles in the fiber forming polymer while maintaining suitable properties for spinning. Among the available fillers, carbon black (CB) and carbon nanotubes (CNT) have been used extensively due to their ability to impart high electrical conductivity to a polymer matrix at relatively low filler content [1, 2, 6, 7]. CB has been used widely in conventional polymer composites due to their relative advantages of low cost, small particle size (high surface area), and aggregation behavior. CB filled

polymer composites in film form have been investigated for various applications including sensors [8], electrodes [9], and electromagnetic interference shielding [10]. However, investigation of CB/polymer composite behavior in fiberweb form has been very limited. CB filled electrospun fiberwebs of various polymers have been investigated to thermally induce color change of electrospun webs [11]. Fiber morphology (such as fineness, length, etc.) and fiberweb structural features such as bond density, etc., as well as the other fiber characteristics determined by interactions between polymer matrix and CB particles have also been found to influence the mechanical properties of nanocomposite fiberwebs [12-14].

Electrospinning provides a convenient route to fabricate fiberwebs of nanofibers. It is a simple process for forming nanoscale to microscale fibers with diameters ranging from tens of nanometers to microns. Numerous experimental and theoretical studies have been published to elucidate the factors such as solution viscosity, solution conductivity, surface tension, and electric field intensity, that markedly influence the morphology of the resulting (nano)fibers and the process itself [15, 16]. Because of the outstanding advantages of nanoscale fibers and relative ease of spinning variety of polymers, electrospun fiberwebs have been evaluated for applications including tissue engineering [17], filtration [18], sensors [19], super hydrophobic surfaces [20],

electrodes in supercapacitors [21], and composite fibers [6, 7, 22].

Polyurethane (PU) has been electrospun by many, primarily to combine its intrinsic properties such as high elasticity and flexibility and advantages of nanofiber [13, 15, 23-25]. The morphology and mechanical behavior of electrospun PU fiberwebs have been investigated in terms of fiber bonding structure [23, 24], and strain-induced orientation [25]. PU has also been electrospun with various fillers to prepare nanocomposite fiberwebs for enhanced mechanical properties [13, 26]. While we have focused exclusively on PU/CB composites, the electrical and other properties of other polymer systems have also been improved by the addition of CB [1, 2].

Percolation theory has been used extensively to investigate composites formed from conducting particles dispersed in an insulating host medium. As the amount of conducting filler material increases the composite undergo an insulator-to-conductor transition when a conducting path is established between two boundaries [1, 2]. A crucial aspect of the fabrication of conductive polymer composites is to understand the minimum amount of conductive filler material for which this conduction occurs which is called the percolation threshold. In general, the percolation threshold should be as low as possible and still allow the composite to fulfill its electrical requirements. In the literature, several processing techniques have been introduced in order to lower the

three-dimensional percolation threshold. These include: multiple percolation (especially double percolation), accumulation of conductive filler at the continuous interfaces of multi-component blends, in situ polymerization of the polymer matrix in the presence of conductive fillers [27, 28]. However, percolation behavior of a deformable fibrous network has not been examined.

The present work in motivated by the lack of reported studies of polymer composites in fiberweb form.   Fiber-based composites of polyurethane (PU), which can potentially be used as compliant electrodes or sensors have been prepared using electrospinning. Their mechanical properties, morphological features, and electrical properties are investigated as functions of filler concentration.

4.3. Experimental

4.3.1. Materials

The thermoplastic ether type polyurethane elastomer (PU, Pellethane 2103-70A) used in this study is a commercially available polymer manufactured by Dow Chemical Co. The conductive filler, carbon black (Ketjenblack® EC-300J) is manufactured by Akzo Nobel. The CBs are characterized by their "structure"; a high-structure CB consists of many primary nanoparticles fused together in a grape-like aggregate. Ketzenblack EC is

a high structure CB composed of prime particles fused into primary aggregates. The diameter of primary carbon particles used in this research is about 30 nm [29].

4.3.2. Specimen Preparation: Compounding and Electrospinning

The composite fiberweb studied in this research was produced by electrospinning [15, 16]. In the electrospinning process, an electric field is used to draw a charged polymer solution or melt from an orifice (usually a syringe tip) to a collector, often a metal plate or screen. As the electric filed is increased, the hemispherical form of the solution or melt droplet held at the end of the orifice is elongated to form a conical shape, which is called Taylor cone. The electric field is increased until it exceeds the surface tension of the first solution drop, exiting the orifice of the spinneret. The electrostatic forces transform the Taylor cone into a continuous jet of polymer from the orifice to the grounded collection device. The discharged polymer jet undergoes a whipping process as the solvent evaporates, to form solid fibers. The fibers are collected on a grounded metal screen in the form of a fiberweb.

The dispersion of CB and the dissolution of the PU/CB composite system for electrospinning were done in a mixture of N,N-dimethylformamide (DMF, Aldrich) and chloroform (Aldrich) (50/50, v/v) at room temperature. First, a stable CB suspension

was obtained by holding CB/DMF/chloroform suspension for one and half hour in an ultrasonic bath (Bransonic, 1510-MTH). Then, PU was dissolved in the stable suspension of CB in DMF/chloroform (50/50, v/v) at room temperature. PU/CB overall weight concentration was fixed at 12.25 wt% to ensure steady electrospinning condition. The concentration of CB was varied between 0 and 9.46 vol% (nominal) to obtain various CB volume concentrations in the composite fiberwebs, while the PU concentrations was altered to keep the overall concentration fixed. Solutions containing higher levels of CB% were found impossible to spin due to high viscosity and discontinuity in flow.

In the electrospinning process, the polymer solution was placed into a syringe with the needle with inner diameter of 0.21 mm. Randomly oriented nanofibers were electrospun by applying a voltage of ~25 kV to the needle using a high voltage supplier (GAMMA, ES30N). The grounded drum collector was located at distance from 20 cm and the polymer solution was fed at a rate of 80 μl/min. by a syringe pump (Kent, GENIE). All electrospun composite fiberwebs produced were dried in vacuum for one week to ensure completely evaporation of solvents. Electrospinning set up used in this research is depicted in Figure 4.1.
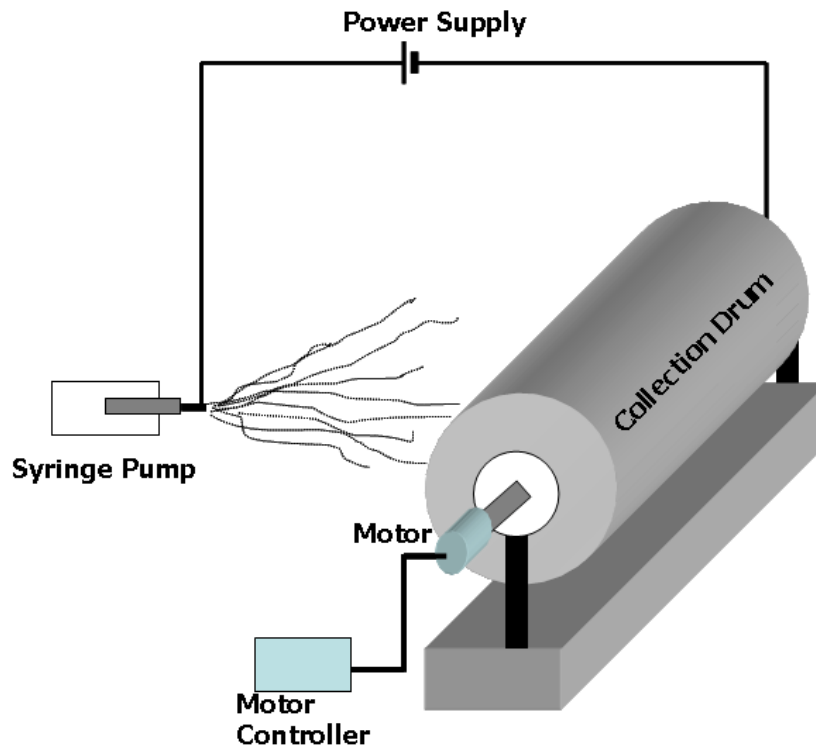
Figure 4.1. Schematic of electrospinning setup consists of collection drum, power supply, and syringe pump.

4.3.3. Solution Topography

Critical properties of polymer composites are influenced by three primary characteristics of the filler: particle size, polymer to filler interaction, and uniformity of particle dispersion [1]. Optimal dispersion is achieved when the CB particles are separated into discrete primary aggregates. During the dispersion-fabrication step, breakdown of aggregates and agglomeration-deagglomeration processes occur, affecting the performance and reproducibility of the composite. High-structure blacks are

especially prone to breakdown. To assess the level of dispersion, the solutions prepared for electrospinning were evaluated in terms of the dispersed particle size using an optical microscope (Olympus BX 60 with PAX-it-M1243 Modulator 20 X software). Figure 4.2 shows topography of 7.47 vol% (nominal) of CB filled solution before electrospinning. It shows that carbon black particles are well dispersed in the solution. Limited analysis of the optical images show aggregate size in the range of 400-1700 nm, indicating efficacy of ultrasonication as a means to disperse CB particles.
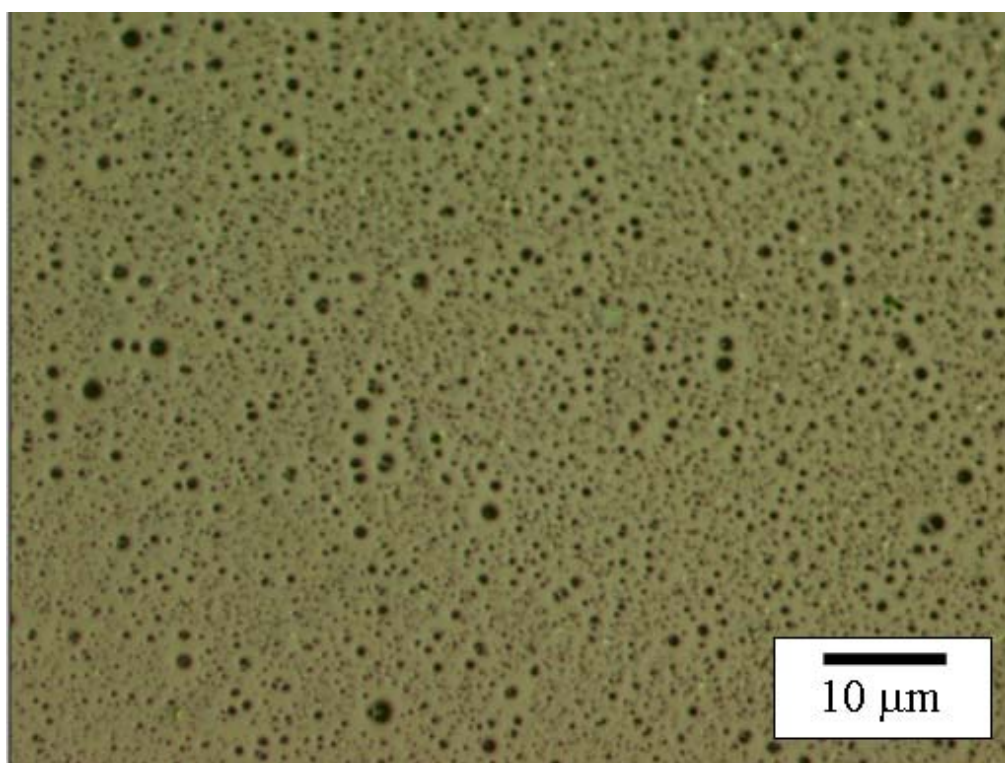
Figure 4.2. Optical micrograph of 7.47 vol% (nominal) of CB filled PU solution in DMF and chloroform (scale marker = 10μm).

4.3.4. Characterization

The electrical conductivity of the fiberwebs was measured at ambient temperature using the standard four point probe technique. A Keithley 220 current source and a Keithley 6517A electrometer were used to measure the current-voltage characteristics of the samples. The sample geometry was used to calculate the resistivity of each sample. The average resistance value of each specimen was obtained from 30 repeated measurements at various positions of the sample. The resistivity ρ of the samples obtained from the measurement was calculated from the following equation,

$$\rho = 4.532t\left(\frac{V}{I}\right)$$

(4.1)

and the conductivity is the reciprocal of equation (4.1). The morphology of the composite fiberwebs was examined by high resolution scanning electron microscopy (Hitachi S-3200 Scanning Electron Microscope). Fiber mean diameter was measured from these images using image analysis software (Image J ver. 1.34s). The measurement of mean diameter was based on the diameter of fibers from 100 different random locations. Thermal stability of the nanofiberwebs were studied by thermo gravimetric analysis (TGA) using a TA instruments' 1000 series thermal analysis

system. All samples were heated from room temperature to 900°C at a scan rate of 10°C/min. in a nitrogen atmosphere. Quasi-static tensile behavior of the fiberwebs was determined using a standard tensile load frame (MTS 30G). In order to normalize load data the samples thicknesses were measured using a micrometer (L&W model 51) at 7.3±0.3 psi normal pressures. The reported values of tensile modulus, strength, and elongation at break are obtained from results of five tests.

4.4. Results and Discussion

4.4.1. Morphological Characteristics and Fiber Diameter

A series of SEM micrographs of nanocomposite fiberwebs with various levels of CB content are presented in Figure 4.3. At higher levels of CB content the fiber surfaces are increasingly irregular and agglomeration of CB particles are apparent on the fiber surfaces, particularly near and beyond the threshold concentrations (Figure 4.3 (b)). The influence of CB content on fiber dimensions and uniformity may not be apparent from the images in Figure 4.3. However, the measured values of fibers diameter and its dispersion presented as a function of filler concentration in Figure 4.4 shows an increase in fiber diameter and greater variability in fiber size distribution for higher CB content. In addition, the images also show higher fiber to fiber bond density for higher CB

content samples. The difference is most likely due to slow rate of solvent evaporation during the fiber formation between the spinneret and the collection surface due to the presence of more CB particles at the higher volume concentrations and their tendency to absorb [30] and thereby slow down the evaporation of solvents. Ketjenblack used in this study is composed of very porous carbon particles with DBP1 value of about 350 cm^3/100g [29]. This CB structure is more likely to absorb and slow down evaporation of solvents. For the same reason, higher resolution images of the fractured nanococmposite fiberwebs show evidence of irregular and sometimes lack of distinct fiber formation in the fiberweb, see Figures 4.3 (g)-(h). These observations are of interest since higher bond density is likely to improve electron transport through the fiberweb.

---

[1] The ratio of dibutylphtalate (DBP)-oil volume that can be absorbed by 100g of CB particles.
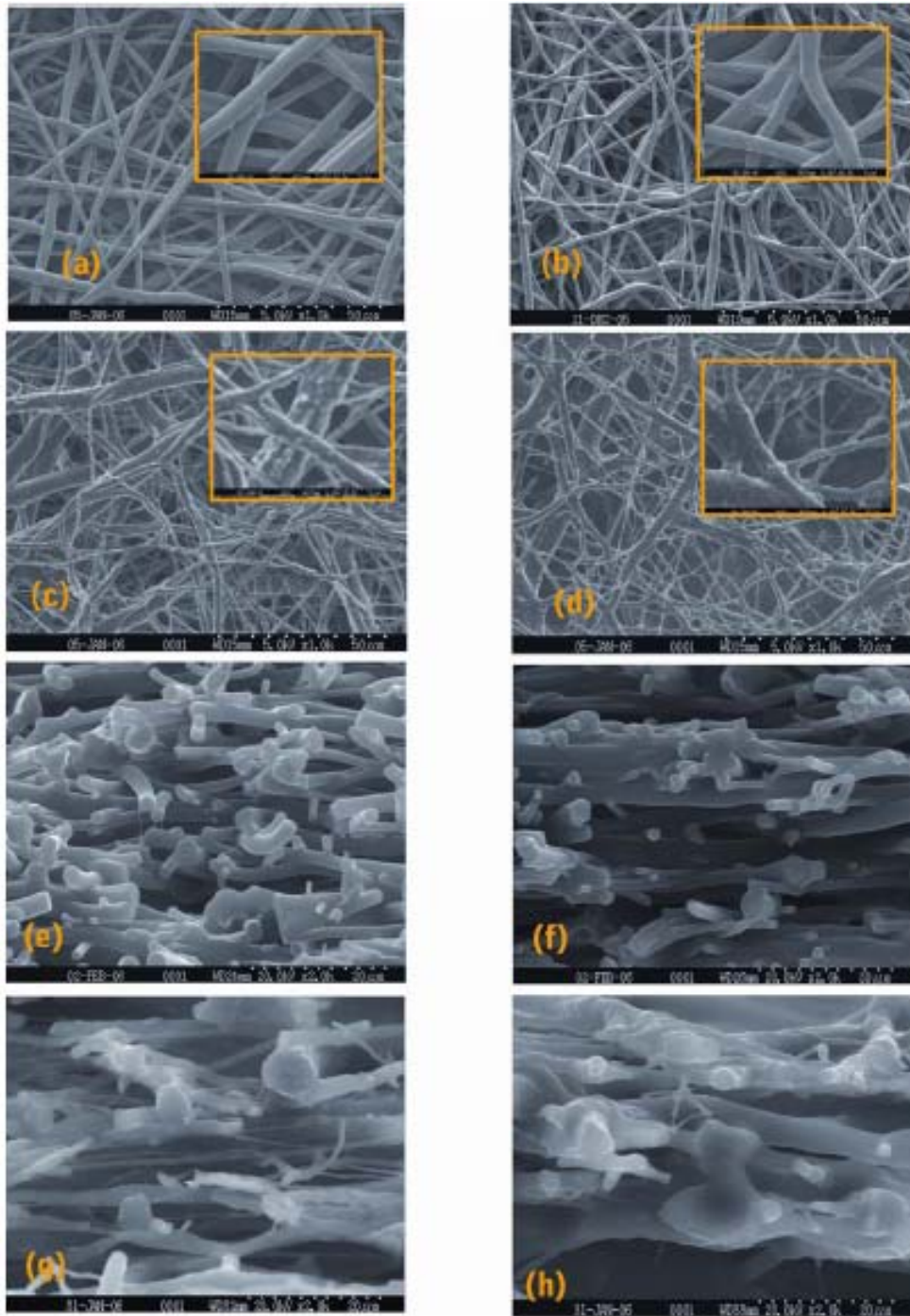
Figure 4.3. Scanning electron micrographs of CB-PU composite electrospun fiberwebs at various CB concentrations (in vol%, nominal, a-d: surface scans, e-h: cryofractured surface): (a) & (e) 0%, (b) & (f) 5.54%, (c) & (g) 7.47%, (d) & (f) 9.46%.
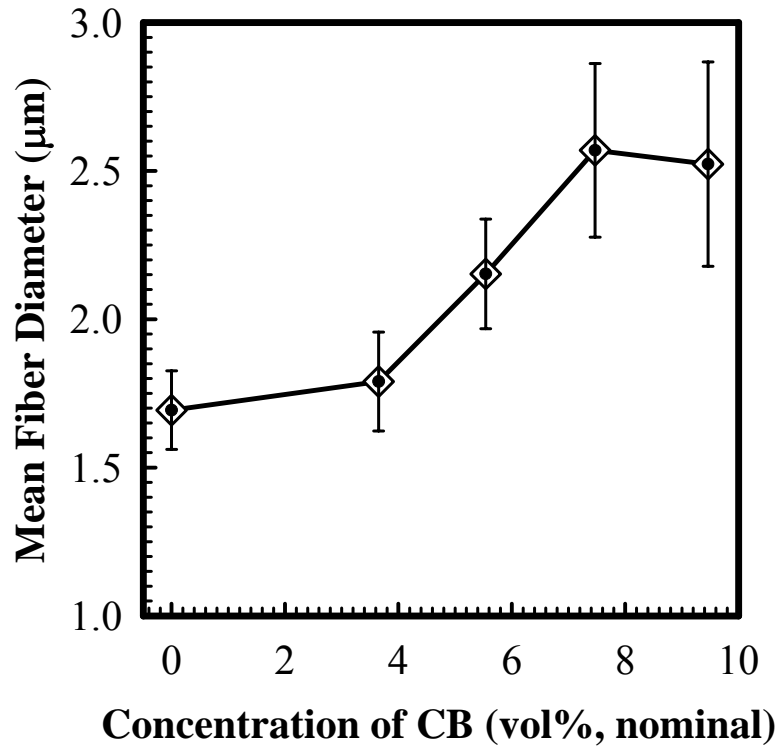
Figure 4.4. Variation of mean diameter of electrospun fibers as a function of nominal CB content (vol%). The error bars correspond to 95% confidence intervals.

4.4.2. Mechanical Properties of the Composite Fiberwebs

Close observation of typical stress-strain curves of various PU/CB nanocomposite fiberwebs presented in Figure 4.5 show some interesting features. The initial modulus of the composite fiberweb increases gradually with increase in CB content; increasing from 0.74 MPa for 0% CB to 1.1MPa for 7.47% CB content. Subsequently, the initial modulus increases about 5 fold to 3.75 MPa at 9.46 vol% (nominal) of filler. In case of

tensile strength, the data presented in Table 4.1 suggests significant improvement at low loadings up to 3.65% of CB, however, at higher concentrations the strength drops below that of the pristine polymer. The extension at failure was found to be highly sensitive to addition of fillers and drops significantly with 1.80% of CB. At higher levels of CB, the values seem to be fluctuating but staying at a low level compared to the elongation at break of fiberwebs with no filler. The overall stress-strain behavior of fiberweb structures found in this study is largely consistent with what has been reported for thermally point bonded nonwovens [31, 32]. The increase in bond density and the over-all area of the bonds for higher CB content as well as the reinforcement effect of high modulus CB particles are likely to improve the modulus of the fiberweb. On the other hand the diminishing strain at failure is most likely caused by the reduced degree of freedom of the fibers due to higher bonding as well as the stiffening of the fibers due to reinforcement. In other studies of electrospun webs, Benli *et al.* [33] reported two fold increase in initial modulus with CB content of 12 wt% in composite films of PU. The addition of CB into various other polymers also generally increased the modulus of the composites [33, 34]. The tensile strength and initial modulus values obtained in this study compares very well with the data reported by Lee *et al* [23]. for electrospun

Pellethane 2363-80AE which is similar in chemical structure to Pellethane 2103-70A

(polyether type urethane) used in this research.

Table 4.1. Tensile behavior of CB-PU composite electrospun fiberwebs. The 95%

confidence intervals are shown with the data.

CB (vol%,nominal)	Initial modulus (MPa)	Tensile Strength (MPa)	Elongation at Break (%)
0.00	0.74±0.16	6.06±1.26	613.51±32.06
1.80	1.03±0.06	6.2±0.96	332.92±35.51
3.65	1.05±0.27	7.48±1.02	322.22±14.51
5.54	1.08±0.10	3.32±0.44	349.51±38.60
7.47	1.10±0.04	3.06±0.24	400.63±15.19
8.46	2.04±0.27	3.82±0.41	350.82±26.45
9.46	3.75±0.86	4.74±0.87	473.51±34.15
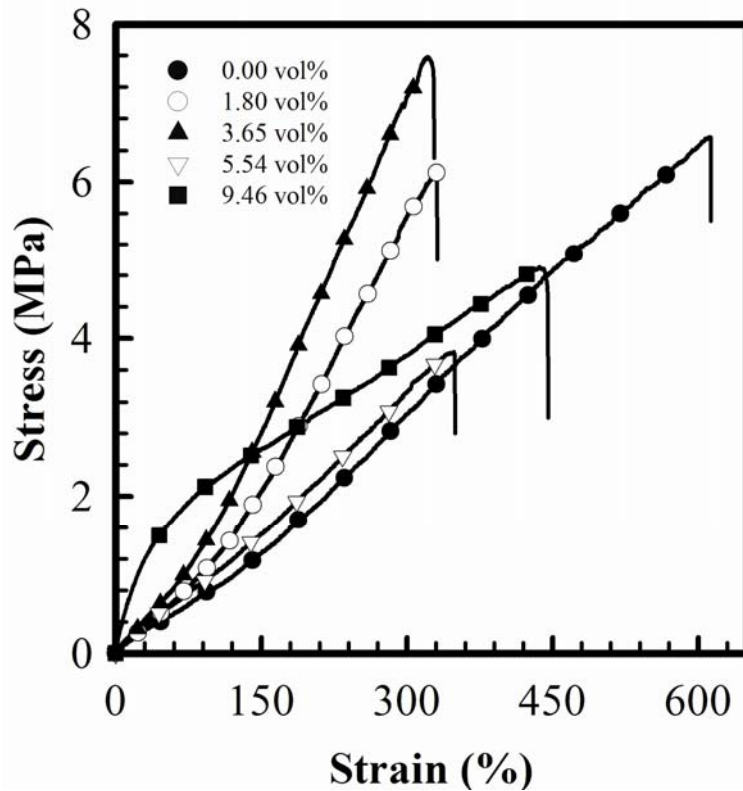
Figure 4.5. Typical stress-strain curves of the CB-PU electrospun fiberwebs at various

filler content (all CB content volume in figure are nominal).

4.4.3 Thermal Analysis

In order to ascertain the CB content as well as to investigate the effects of CB on

thermal stability of the composite fiberweb, thermo-gravimetric analysis (TGA) was

performed on all composite samples. The changes in weight of various CB/PU

fiberwebs as a function of temperature are plotted in Figure 4.6. Close examination of

the TGA data presented in Figure 4.6 and Table 4.2 show improved thermal stability of

the composite fiberweb with relatively low CB content up to 5.54 vol% (nominal). The

decomposition temperature is noted at 284°C with 5.54 vol% (nominal) of CB

compared to 276°C for the pristine polymer fiberweb. However, with subsequent

increase of CB content to 7.47 vol% (nominal) and higher the decomposition temp

reduced to 269°C and lower. Thermal stability is generally expected to improve with the

incorporation of more thermally stable fillers such as CNT and CF into fibers [35, 36],

additionally, as argued by Shaffer *et al*. [37] for CNT composite, the adsorption of free

radicals by the CNT surface may help improve thermal stability. The reason for

lowering of thermal stability at higher CB loadings is not clear. However it could be due

to the agglomeration of CB at higher loadings. Similar results have been reported in the

literature for CNT-polymer composites [37, 38], and organoclay-polymer composite

[39].
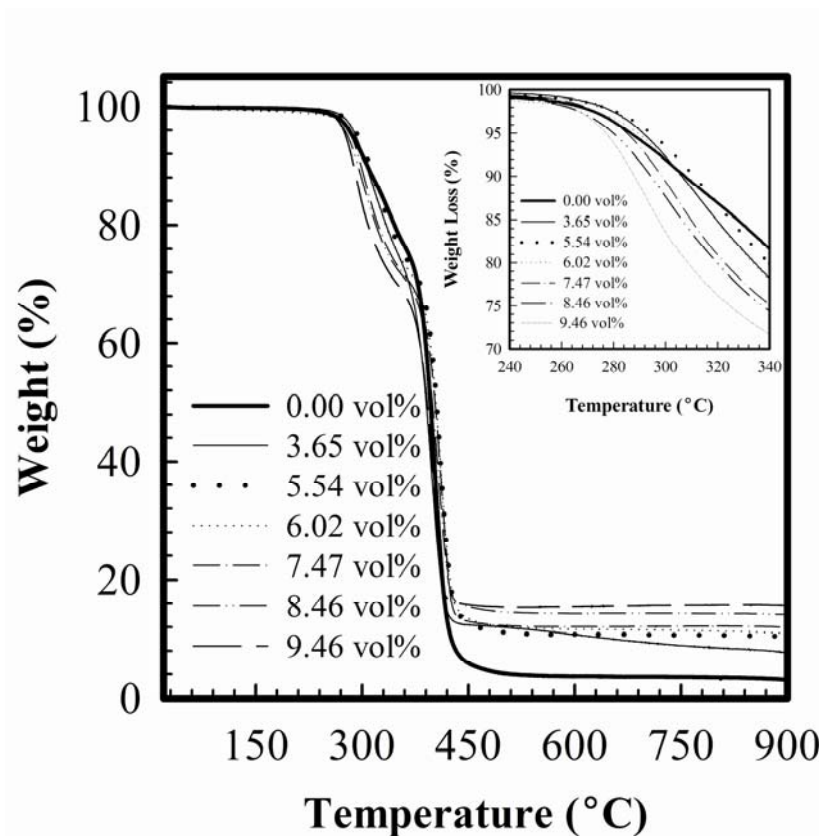
Figure 4.6. TGA of CB-PU electrospun fiberwebs in nitrogen atmosphere. The inset shows the onset of decomposition, in detail (all CB content volume in figure are nominal).

The mass loss due to CB oxidation was minimized by the nitrogen environment in which the TGA was carried out, while PU matrix thermally decomposed almost completely after being heated to 900°C. The masses remaining are almost entirely due to the CB and the actual CB content of various fiberwebs was computed from the residues. The results are summarized in Table 4.2. Actual weight fractions of CB in the

fiberwebs are found to be significantly lower than their nominal values. The most likely

reason is the loss of CB particles during the preparation of CB suspension and

subsequent mixing with the polymers followed by electrospinning from a syringe. Even

with continuous agitation during the processing a small amount of CB precipitated,

causing a lower actual CB content in the fiberweb.

Table 4.2. Decomposition temperature of various CB-PU composite electrospun

fiberwebs and actual CB content determined from TGA.

Nominal CB Content, wt% (vol%)	Measured CB Content, wt% (vol%)	Decomposition Temperature (a) (°C)
0.00 (0.00)	0.00 (0.00)	276.40
5.88 (3.65)	4.66 (2.87)	283.18
8.82 (5.54)	7.35 (4.58)	284.35
9.56 (6.02)	7.87 (4.92)	277.90
11.76 (7.47)	8.90 (5.58)	276.60
13.23 (8.46)	11.02 (6.98)	270.50
14.71 (9.46)	12.60 (8.03)	269.70

(a): temperature at 3 wt% loss

4.4.4. Electrical Conductivity and Percolation Behavior

The variation in DC conductivity of the nanocomposite fiberwebs with respect to filler

concentration is shown in Figure 4.7. The conductivity of pure PU fiberweb was measured at about 1.14×10^{-7} S/cm. A sharp increase in conductivity of approximately 3 orders of magnitude was recorded between 5.54 and 6.02 vol% (nominal) filler content. As the filler concentration increased from 5.54 and 6.02 vol% (nominal) the conductivity increased from about 1.88×10^{-7} S/cm to about 6.80×10^{-5} S/cm. After that the conductivity changed only moderately, increasing to about 1.07×10^{-2} S/cm for 9.46 vol% (nominal) filler content. This behavior is indicative of a percolation transition. As seen in Figure 4.7, the percolation threshold of the PU/CB nanocomposite fiberweb lies between 5.54 and 6.02 vol% (nominal) of nominal CB. In light of TGA data presented earlier, this represents an actual CB content between 4.58 and 4.92 vol%. Percolation threshold for various CB composites including PU/CB composites have reported to be in the range of 2-12 vol% [40-42].

The electrical conductivity of a composite (σ_c) above the percolation threshold can be expressed as [43]

$$\sigma_c = \sigma_0(f - f_c)^t \qquad for \ \ f > f_c \tag{4.2}$$

where σ_0 is the constant of proportionality, f is the volume fraction of the conducting filler in the composite, and f_c is the critical volume fraction (volume fraction at

percolation), and t is a critical exponent. The value of the critical exponent t is expected to be material independent [44] and considered indicative of the "strength" of the percolation transition. For any three dimensional system the exponent t yields a value of about 2.0 [45]. Analysis of our data presented in the inset of Figure 4.7 resulted in a value for t of 2.165, when the percolation threshold is assumed as 4.6 vol%. The inset of Figure 4.7 shows a plot of our data in the form of the power law relation of equation (4.2). The value of the critical exponent, t, is in line with what has been reported in the literature for CB-filled polymer composites and in particular for high structure carbon black filled composites [46]. Detailed investigation of the seemingly tunneling-percolation behavior of the CB-PU composite in the fiberweb form remains a subject of investigation.
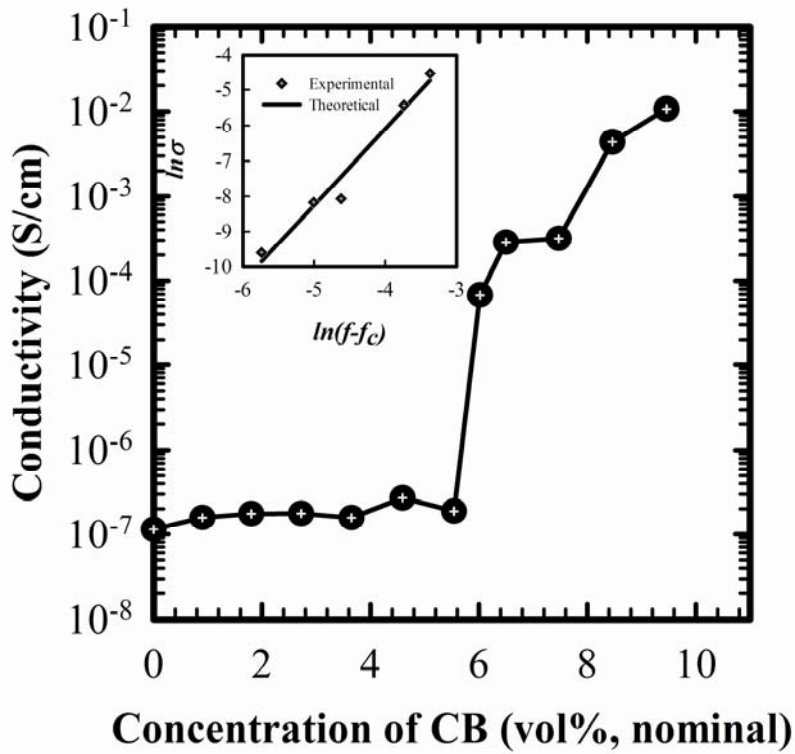
Figure 4.7. Electrical conductivity of the PU-CB electrospun fiberweb as a function of filler content. Inset shows the fit of the experimental data to the power law of percolation (equation 4.2).

4.5. Conclusions

The report describes a successful and unique route for fabricating porous conducting composite fiberwebs containing carbon blacks. The results clearly demonstrate the efficacy of incorporating CB into the PU matrix using electrospinning. The influence of higher CB content on the electrospun fibers manifested in larger fibers as well as higher

bond density. The initial modulus of the fiberweb increased substantially with increasing CB content. The presence of CB increased fiberweb strength marginally up to 3.65 vol% (nominal) CB content and fell significantly beyond that. Electrical conductivity, as well as thermal stability increased significantly up to about 5.54 vol% (nominal) of CB. The electrical conductivity of the composite fiberweb has been found to increase about 3 orders of magnitude when the filler content increased from 5.54 vol% to 6.02 vol% (nominal). The percolation threshold of conductivity was determined to be between 4.58-4.92 vol% of CB.   The critical exponent of percolation (t) was calculated as 2.165, when the percolation threshold was assumed to be around 4.6 vol%. The results seem to confirm the tunneling-percolation behavior of the CB-PU composite fiberweb investigated in this research.

4.6. References

1.   Huang, J., *Carbon Black Filled Conducting Polymers and Polymer Blends.* Adv Polym Technol, 2002. **21**: p. 299.

2.   DDL, C., *Review Electrical Applications of Carbon Materials.* J Mater Sci, 2004. **39**: p. 2645.

3. Thosenson, E.T., Ren, Z., and Cou, T., *Advances in the Science and Technology of Carbon Nanotubes and Their Composites: a Review.* Compos Sci and Technol, 2001. **61**: p. 1899.

4. Calvert, P., *A Recipe for Strength.* Nature, 1999. **399**: p. 210.

5. Kang, T.S., Lee, S. W., Joo, J., and Lee, J. Y., *Electrically Conducting Polypyrrole Fibers Spun by Electrospinning.* Synth Met, 2005. **153**: p. 61.

6. Munoz, E., Suh, D., Collins, S., Selvidge, M., Dalton, A. B., Kim, B. G., Razal, J. M., Ussery, G., Rinzler, A. G., Martinez, M. T., and Baughman, R. H., *Highly Conducting Carbon Nanotube/Polyethylene Composite Fibers.* Adv Mater, 2005. **17**: p. 1064.

7. Seoul, C., Kim, Y., and Baek, C., *Electrospinning of Poly(vinylidene-fluoride)/Dimethylformamide Solutions with Carbon Nanotubes.* J Polym Sci, Part B: Polym Phys, 2003. **41**: p. 1572.

8. Chen, S.G., Hu, J. W., Zhang, M. Q., Rong, M. Z., and Zheng, Q., *Improvement of Gas Sensing Performance of Carbon Black/Waterborne Polyurethane Composites: Effects of Crosslinking Treatment.* Sens Actuators, B, 2006. **113**: p. 361.

9.   Richner R, M.S., Wokaun A, *Grafted and Crosslinked Carbon Black as an Electrode Material for Double Layer Capacitors.* Carbon, 2002. **40**: p. 307.

10.   Bigg DM, S.D., *Plastic Composites for Electromagnetic Interference Shielding Applications.* Polym Compos, 1983. **4**: p. 40.

11.   Pedicini, A., and Farris, R. J., *Thermally Induced Color Change in Electrospun Fiber Mats.* J Polym Sci, Part B: Polym Phys, 2004. **42**: p. 752.

12.   Inai, R., Kotaki, M., Ramakrishna, S, *Deformation Behavior of Electrospun Poly(L-lactic-co-ε-caprolactone) Nonwoven Membranes under Uniaxial Tensile Loading.* J Polym Sci, Part B: Polym Phys, 2005. **43**: p. 3205.

13.   Hong, J.H., Jeong, E. H., Lee, H. S., Baik, D. H., Seo, S. W., and Youk, J. H., *Electrospinning of Polyurethane/Organically Modified Montmorillonite Nanocomposites.* J Polym Sci, Part B: Polym Phys, 2005. **43**: p. 3171.

14.   Choi, S.S., Lee, S. G., Joo, C. W., Im, S. S., Kim, S. H., *Formation of Interfiber Bonding in Eelectrospun Poly(Etherimide) Nanofiber Web.* J. Mater. Sci., 2004. **39**: p. 1511.

15.   Theron, S.A., Zussman, E., and Yarin, A. L., *Experimental Investigation of the Governing Parameters in the Electrospinning of Polymer Solutions.* Polymer, 2004. **45**: p. 2017.

16. Fridrikh SV, Y.J., Brenner MP, Rutledge GC, Phys Rev Lett, 2003. **90**: p. 144502.

17. Xu, C.Y., Inai, R., Kotaki, M., and Ramakrishna, S., Biomaterials, 2004. **25**: p. 877.

18. Tsai PP, S.-G.H., Gibson P, *Different Electrostatic Methods for Making Electret Filters.* J Electrostatics, 2002. **54**: p. 333.

19. Kessick R, T.G., *Electrospun Polymer Composite Fiber Arrays for the Detection and Identification of Volatile Organic Compounds.* Sens Actuators, B, 2006. **Article in press**.

20. Ma M, M.Y., Gupta M, Gleason KK, Rutledge GC, *Superhydrophobic Fabrics Produced by Electrospinning and Chemical Vapor Deposition.* Macromolecules, 2005. **38**: p. 9742.

21. Kim, C., and Yang, K. S., *Electrochmical Properties of Carbon Nanofiber Web as an Electrode for Supercapacitor Prepared by Electrospinning.* Appl. Phys. Lett, 2003. **83**: p. 1216.

22. Ge, J.J., Hou, H., Li, Q., Graham, M. J., Greiner, A., Reneker, D. H., Harris, F. W., and Cheng, S. Z. D., *Assembly of Well-Aligned Multiwalled Carbon Nanotubes in Confined Polyacrylonitrile Environments: Electrospun Composites Nanofiber Sheets.* J. Am. Chem. Soc., 2004. **126**: p. 15754.

23. Lee, K.H., Kim, H. Y., Ryu, Y. J., Kim, K. W., and Choi, S. W., *Mechanical Behavior of Electrospun Fiber Mats of Poly(vinyl chloride)/Polyurethane Polyblends.* J Polym Sci, Part B: Polym Phys, 2003. **41**: p. 1256.

24. Kidoaki, S., Kwon, I. K., and Matsuda, T., *Structural Feature and Mechanical Properties of In Situ-Bonded Meshes of Segmented Polyurethane Electrospun from Mixed Solvents.* J. Biomed. Mater. Res, Part B: Appl. Biomater., 2006. **76B**(1): p. 219.

25. Pedicini, A., and Farris, R. J., *Mechanical Behavior of Electrospun Polyurethane.* Polymer, 2003. **44**: p. 6857.

26. Sen, R., Zhao, B., Perea, D., Itkis, M. E., Hu, H., Love, J., Bekyarova, E., and Haddon, R. C., *Preparation of Single-Walled Carbon Nanotube Reinforced Polystyrene and Polyurethane Nanofibers and Membranes by Electrospinning.* Nano Lett., 2004. **4**: p. 459.

27. Gubbels F, J.R., Teyssie Ph, Vanlathem E, Deltour R, Calderone A, Parente V, Bredas JL, *Selective Localization of Carbon Black in Immiscible Polymer Blends: A Useful Tool To Design Electrical Conductive Composites.* Macromolecules, 1994. **27**: p. 1972.

28. Thongruang W, S.R., Balik CM, *Bridged Double Percolation in*

ConductivePolymer Composites: an Electrical Conductivity, Morphology and Mechanical Property Study. Polymer, 2002. **43**: p. 3717.

29. Mallette JG, Q.L., Marquez A, Manero O, *Carbon Black-Filled PET/HDPE/ Blends: Effect of the CB Structure on Rheological and Electric Properties.* J Appl Polym Sci, 2001. **81**: p. 562.

30. Lawandy SN, W.M., *Penetration of Oils into Polychloroprene Rubber.* J Appl Polym Sci, 1990. **40**: p. 323.

31. Michielsen S, P.B., Desai P, *Review of Thermally Point-Bonded Nonwovens: Materials, Processes, and Properties.* J Appl Polym Sci, 2006. **99**: p. 2489.

32. Batra SK, D.H., Dharmadhikary RK, Gilmore TF, *Influence of Fiber Structure on Properties of Thermally Point-Bonded Polypropylene Nonwovens.* Text Res J, 1999. **69**: p. 725.

33. Benli S, Y.U., Pekel F, Ozkar S, *Effect of Fillers on Thermal and Mechanical Properties of Polyurethane Elastomer.* J. Appl. Polym. Sci., 1998. **68**: p. 1057.

34. Flandin, L., Hiltner, A., and Baer, E., *Interrelationships between Electrical and Mechanical Properties of a Carbon Black-Filled Ethylene-Octene Elastomer.* Polymer, 2001. **42**: p. 827.

35.	Wang, Y., Cheng, R., Liang, L., and Wang, Y., *Study on the Preparation and Characterization of Ultra-High Molecular Weight Polyethylene–Carbon Nanotubes Composite Fiber.* Compos Sci Technol, 2005. **65**: p. 793.

36.	Ma, H., Zeng, J., Realff, M. L., Kumar, S., and Schiraldi, D. A., *Processing, Structure, and Properties of Fibers from Polyester/Carbon Nanofiber Composites.* Compos Sci Technol, 2003. **63**: p. 1617.

37.	Shaffer MS, W.A., *Fabrication and Characterization of Carbon Nanotube/Poly(vinyl alcohol) Composites.* Adv Mater, 1999. **11**: p. 937.

38.	Velasco-Santos, C., Martinez-Hernandez, A. L., Fisher, F., Ruoff, R., and Castano, V. M., *Dynamical-Mechanical and Thermal Analysis of Carbon Nanotube-Methyl-Ethyl Methacrylate Nanocomposites.* J. Phys. D: Appl. Phys., 2003. **36**: p. 1423.

39.	Chang JH, P.D., *Nanocomposites of Poly(ethylene terephthalate-co-ethylene naphthalate) with Organoclay.* J Polym Sci, Part B: Polym Phys, 2001. **39**: p. 2581.

40.	Xiong C, Z.Z., Xu W, Hu H, Zhang Y, Dong L, *Polyurethane/Carbon Black Composites with High Positive Temperature Coefficient and Low Critical Tansformation Temperature.* Carbon, 2005. **43**: p. 1778.

41. Heiser JA, K.J., Konell JP, Sutter LL., *Electrical Conductivity of Carbon Filled Nylon 6,6.* Adv. Polym. Tech., 2004. **23**(2): p. 135.

42. Flandin, L., Chang, A., Nazarenko, S., Hiltner, A., and Baer, E., *Effect of Strain on the Properties of an Ethylene–Octene Elastomer with Conductive Carbon Fillers.* J. Appl. Polym. Sci., 2000. **76**: p. 894.

43. Kirkpatrick, S., *Percolation and Conduction.* Rev. Mod. Phys., 1973. **45**: p. 574.

44. Stauffer D, A.A., *Introduction to Percolation Theory.* 1994.

45. Batrouni GG, H.A., Larson B, *Current Distribution in the Three-Dimensional Random Resistor Network at the Percolation Threshold.* Phys. Rev. E, 1996. **53**: p. 2292.

46. Balberg, I., *A Comprehensive Picture of the Electrical Phenomena in Carbon Black–Polymer Composites.* Carbon, 2002. **40**: p. 139.

CHAPTER 5.

ELECTRICAL PROPERTIES OF FLEXIBLE

NANOCOMPOSITE FIBERWEBS

5.1. Abstract

Carbon black filled composite polyurethane fiberwebs were fabricated by electrospinning to produce electrically conductive, porous, flexible, elastic conducting fiberwebs suitable for many applications including sensors and self monitoring substrates. The piezoresistive gauge factor, current voltage characteristics and percolation thresholds of the electrospun films were compared with spin cast thin films of the same volume percentage of carbon black. It was found that the electrospun webs had more linear current voltage relationship than spin cast films. The fiberweb composite materials were also applied to electroactive polymers to form actuators with a mean actuation response of 12.7 percent. The piezoresitive nature of the fiberweb composite shows potential for self monitoring applications.

Key words: Piezoresistance; Carbon Black; Dielectric Actuator: Electrospun composite polyurethane fiberweb;

5.2. Introduction

There is a significant and increasing interest in developing lightweight and deformable conductive materials for use in flexible electronics including self-monitoring substrates and flexible electrodes. The formation of durable electrodes that can withstand large strains remains a major challenge. Furthermore, it is of interest, to be able to monitor the strain of such devices while they undergo deformation.

Electrospun fiberwebs have been investigated and in some cases commercially used for tissue engineering [1], filtration [2], sensors [3], super hydrophobic surfaces [4], electrodes in supercapacitors [5], etc. The network of deposited nanofibers forms a porous, flexible structure with very large surface area. Incorporation of conductive fillers such as carbon black or carbon nanotubes into the starter polymer solution results in the formation of conductive nanocomposite fibers [6-8] making a deformable electrically conductive structure that is mechanically robust. The electrical conductibility of electrospun fiberweb is dependent on the amount of conductive filler material in the polymer matrix. Below a critical level of particle content, known as percolation threshold, the particles are not in contact, or are too far way from each other for quantum tunneling to occur, and the material is essentially insulating. Above the

percolation threshold there are sufficient numbers of particles in contact such that a continuous pathway for conduction is formed.

The name 'piezo' comes from the Greek word 'piezin' which means squeezing or pressing tightly. Combined with resistivity it describes the dependence of electrical resistivity of a material on applied mechanical stress or strain. For a composite near the critical threshold, we would expect to see a piezoresistive effect. Beyond the percolation threshold the conducting particles in a composite are sufficiently close to each other to manifest low resistivity. As a stress (tensile) is applied on the composite, the elastic polymer matrix deforms to the extent that the conducting filler particles are forced farther from each other breaking existing conduction paths, resulting in higher resistivity. Thus knowledge of this change in resistivity may allow measurement of the strain experiences by the composite. Consequently, the understanding of elastic properties of the composites is very important in order to design pressure sensors. Because of this simplicity, piezoresistivity is one of the most often used transducer effects. Piezoresitive materials have been used in self sensing systems for the monitoring structural integrity and in biomonitoring devices [9].

The sensitivity of piezoresistivity can be evaluated by the gauge factor (GF). It has been previously observed in composite materials that large values of piezoresistive sensitivity

(the gauge factor) in RuO_2-glass thick-film resistors are obtained when tunneling is the mechanism of electrical conductivity [10, 11]. When the piezoresistance material is under tension, tunneling distance and/or the distance between fillers can be extended and the resistance decreases strongly due to the exponential nature of the tunneling process. Similarly, viewing the particles as a network of hard spheres in contact, when the material undergoes strain the conductivity decreases when the number of continuous pathways for conduction is decreased.

Piezoresistive composite materials generally consist of conducting fillers and polymer matrix. Conductive filler materials such as carbon fiber [12-17] carbon nanotubes,[18] and graphite nanosheets [19, 20] are considered as a promising filler material because the high aspect ratio of material itself. The high aspect ratio contributes to the advantages of forming a conducting network at a relatively low contents and leads to a higher conductivity which is related to the sharp sensitivity of the piezoresistivity. Out of these fillers, carbon fiber filled composite has been used often in piezoresistive strain sensor materials because their stress-strain behavior is linearly elastic and shows relatively high piezoresistive response [15, 16]. In comparison the piezoresistive response of carbon black filled composite has been more limited [21-23]. This may be due to the spherical form of particles and tendency to form

agglomerates, leading to deterioration of material properties. In addition to the shape of the conductive filler material, other factors such as the applied stress, filler morphology, filler spatial arrangements, filler volume fraction, and tunneling distance can influence the piezoresistive response [23]. The Young's modulus of matrix material is another important factor. Piezoresistivity of the materials can be increased if more flexible polymer matrix is used [24, 25].

In the present study, our goal is to investigate the electrospun composite fiberweb as a self-monitoring, piezoresistive material. We also intend to evaluate the electrospun composite fiberwebs in a suitable application as electrodes for an electroactive polymer actuator. Electrospun fiberweb with carbon black content above the percolation threshold were found to be suitable for compliant electrodes showing actuation response even though fiberwebs possess high porosity. A comparison of the electrical properties of spin cast films with electrospun fiberweb was also performed.

5.3. Experimental

5.3.1. Materials

The thermoplastic polyurethane elastomer (PU, Pellethane 2103-70A) used in this study is a commercially available polymer manufactured by Dow Chemical Co. The

conductive filler, carbon black (Ketjenblack® EC-300J) is manufactured by Akzo Nobel. Carbon blacks are characterized by their "structure"; a high-structure carbon black consists of many primary nanoparticles fused together in a grape-like aggregate. Ketzenblack EC is a high structure carbon black composed of prime particles fused into primary aggregates. The diameter of primary carbon particles used in this research is about 30 nm [26].

5.3.2. Specimen Preparation: Compounding and Electrospinning

The composite fiberweb studied in this research was produced by electrospinning [27, 28] and the dispersion and electrospinning procedure was similar to the procedure in the former chapter. Films have been prepared using spin-casting for 3 min. at 700 RPM. Dimension of 25×25 mm^2 of glass slides were used as a substrates. All films were also dried in vacuum for one week to ensure complete evaporation of solvents.

5.3.3. Characterization

Electrically conductive fiberwebs and spin cast films were characterized for their electrical and mechanical behaviors. The electrical conductivity of the fiberwebs was measured at ambient temperature using the standard four point probe technique. A

Keithley 220 current source and a Keithley 6517A electrometer were used to measure the current-voltage characteristics of the both samples. The sample geometry was used to calculate volume resistivity of each sample. The average resistance value of each specimen was obtained from 30 repeated measurements at various positions of the sample. I-V characteristics of films and fiberwebs were investigated using HP 4212B. Currents were measured as voltage increases from -20 to 20 V with identical probe positions.

Quasi-static tensile behavior of the fiberwebs and films were determined using a standard tensile load frame (MTS 30G). In order to normalize load data the samples thicknesses were measured using a micrometer (L&W model 51) at 7.3±0.3 psi normal pressures. The reported values of tensile modulus are obtained from results of five tests. To quantify an important physical characteristic that is significantly different for the fiberwebs and films the porosity (void volume/total volume) values of the fiberwebs were calculated.

All samples of fiberwebs were cut into dimension of 10×40 mm^2 and 4 samples were used in each piezoresistance testing. The dimension of films were 25×25 mm^2 and 4 samples are prepared as well. For the samples, 7.47, 8.46, 9.46 vol% (nominal) of carbon black filled composite fiberwebs and films were used in order to prevent large

fluctuations in resistance and to maximize the gauge factor [25]. The piezoresistance measurements were done by measuring the electrical resistance R under constant uniaxial strain from 0 to 60% with step-wise increase of 10% produced by a custom-built instrument. Samples were placed on each side of the mounts of micro-strain instrument. Fixed dimension of four probes are adhered to the samples directly to measure the voltage changes with applied currents. The electrical resistance of the fiberwebs and films was measured at ambient temperature using the standard four point probe technique. A Keithley 6221 current source and a Keithley 2182A nanovoltmeter were used to measure the current-voltage characteristics of the samples. The reported values of resistance changes, fractional resistance changes ($\Delta R/R_0$), and gauge factors (GF) are obtained from average results of four tests.

5.3.4. Applications of Fiberweb as an Electrode: Actuation Testing

Dielectric polymer actuators require electrodes for actuation [29]. The electrospun nanocomposite fiberweb has been investigated as electrodes in such actuators. Figure 5.1 illustrates the principle of operation of a dielectric polymer actuator showing the effect of applied voltage on a dielectric elastomeric polymer film sandwiched between two compliant electrodes. When a voltage is applied between the electrodes, the

polymer is squeezed in thickness and stretched in length and width by the electrostatic forces.

To carry out this test, diaphragm actuator was fabricated. Diaphragm actuator consists of two composite fiberwebs as electrodes and medium, a commercially available acrylic foam tape (VHB TM 4910, 3M Corp.) as the dielectric, which is stretched under uniform nominal pre-strain (250% in both X and Y directions). Electric potential up to 20 kV was applied to the diaphragm actuator. Actuation process was recorded as a video file and analyzed the actuation response using image analysis software (Matrox Inspector ver 4.1). Actuation response was characterized by the areal strain. Areal strain was calculated by the equation below.

$$Areal\ strain = \frac{actuated\ area - unactuated\ area}{unactuated\ area} \times 100(\%)$$

(5.1)
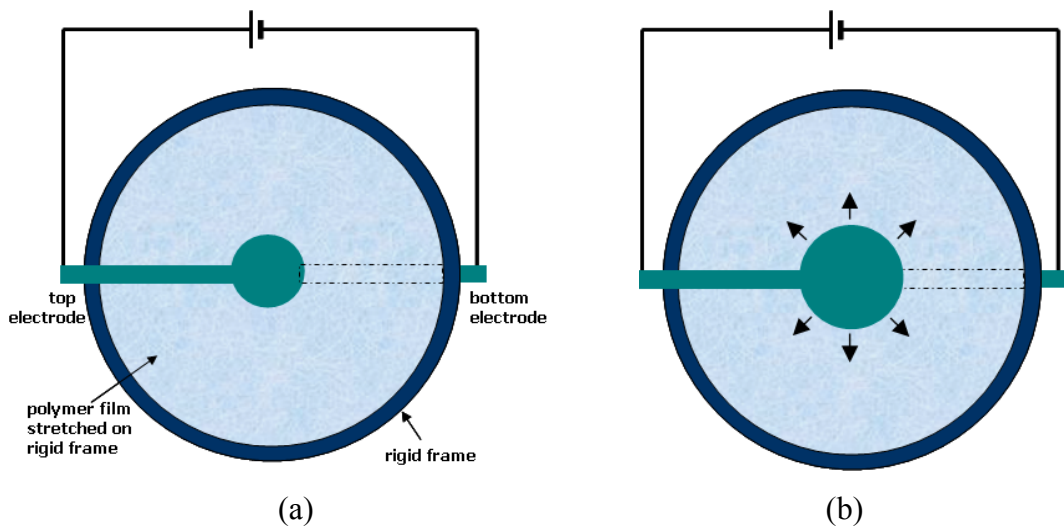
Figure 5.1. Schematic illustration of the operation of dielectric polymer actuator: (a) voltage off, and (b) voltage on.

5.4. Results and Discussion

5.4.1. Electrical Behavior

Figure 5.2 shows the conductivity of the films and fiberwebs as a function of filler content. For both fiberweb and film, the percolation threshold was found to be around 4.7 vol% of CB. However, the conductivity of films at higher loadings of carbon black is lower than that of comparable electrospun fiberwebs. This observation is very limited, however, Yamashita *et al.* [30] also reported that the electrical conductivity of carbon nanofiber filled elastomeric nonwoven produced by electrospinning is higher than the cast film because of the oriented carbon nanofiber in the nonwoven. Thus, this higher conductivity of the fiberweb may be due to the higher surface area of fiberwebs than the

films and the difference in carbon black distribution within the matrix, or alignment of

the carbon black during the electrospinning process.
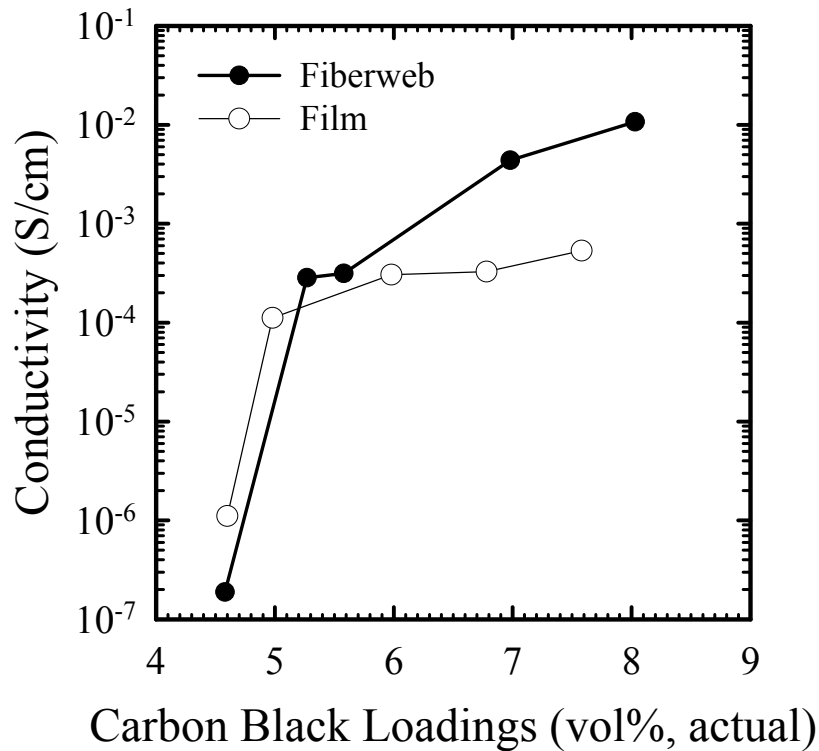
Figure 5.2. Electrical conductivity of the nanocomposite electrospun fiberweb and spin

cast nanocomposite film as a function of actual filler content measured by TGA.

Percolation threshold for both materials are considered as 4.7 vol% of CB.

The current-voltage (I-V) curves for both spin-cast film and electrospun fiberweb

with 6.5 vol% (nominal) loading are shown in Figures 5.3 (a) & (b) respectively. In

each graph a sequence of I-V sweeps from -20 to +20 V are shown. At high absolute

values of voltage (i.e. from +15-20V) the current increases linearly, while for low

voltages the current values are substantially smaller as a result the curve looks

somewhat diode-like. Furthermore on subsequent sweeps one finds that the resistance is

lowered, and the curve becomes more linear over the whole voltage range. Similarly

one finds the same behavior in Figure 5.3 (c) for the 7.47 vol% (nominal) carbon black

loaded fiberweb except that the lower voltage region is smaller. This suggests that the

initial formed percolation network can be altered by the application of high voltage.

Initially at low voltages, particles in contact form the network, and as the voltage is

increased quantum tunneling play a more significant role to the current contribution. As

the voltage is increased, it is likely that the very thin polymer barrier between closely

positioned particles is broken down by the high field between particles. Like many

dielectric breakdowns, this breakdown appears to be irreversible and thus on subsequent

sweeps the conductivity of the material is found to be higher. In addition, both

fiberwebs and films show non-Ohmic behavior. This non-Ohmic behavior of

composites are reported elsewhere and it is due to the quantum tunneling conduction

mechanism in the percolation threshold regime [31, 32]. However, fiberwebs show

more linear I-V curve than the films. This can be attributed to wider distribution of

inter-particle distances of films than fiberwebs. According to Balberg [33], tunneling

conductance with the inter-particle distance follows exponential decay. In addition, a

wide distribution of the inter-particle distances can result in diverging distribution of

high resistance elements in network [34]. From this argument we can think that films

may have wider distribution of inter-particle distance, leading to more non-Ohmic

behavior than the fiberweb. Moreover Balberg also suggested that average inter-particle

distance can be different in different networks [34].
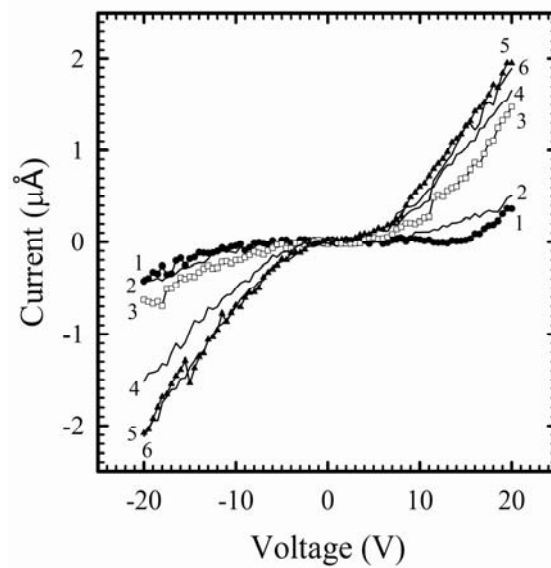
(a)
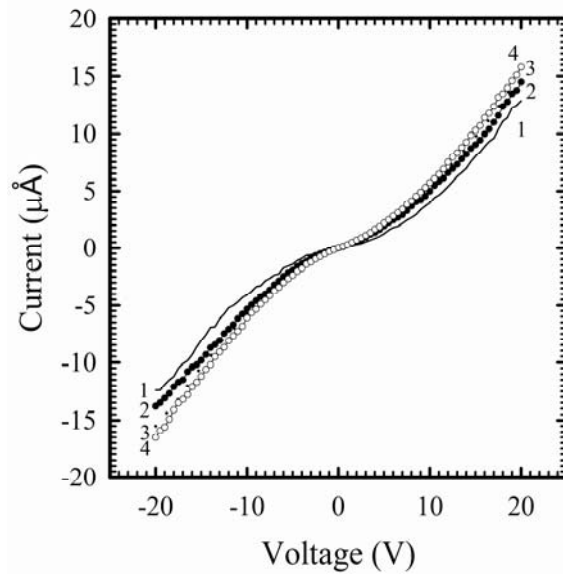
(b)
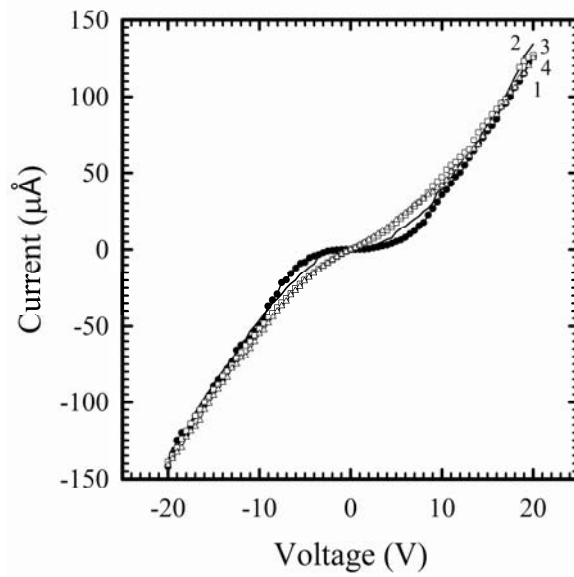
(c)

Figure 5.3. I-V relation of various loadings of carbon black filled films and fiberwebs

(in vol%, nominal): (a) 6.5 vol% CB filled film, (b) 6.5 vol% CB filled fiberweb, and

(c) 7.47 vol% CB filled fiberweb. Fiberwebs show more linear I-V relation than the film.

Initial modulus of fiberwebs and films are summarized in Table 5.1. Films show much higher modulus as well as wider distribution of modulus than the fiberwebs at same loadings of CB, indicating that fiberwebs are much flexible. Figure 5.4 shows the tensile behavior of fiberwebs and films at 8.46 vol% (nominal) of carbon black loadings.

Table 5.1. Tensile behavior of CB-PU electrospun composite fiberwebs and spin cast films. The 95% confidence intervals are shown with the data.

Volume Concentration of CB (nominal, vol%)	Modulus of Electrospun Fiberwebs (MPa)	Modulus of Spin Cast Films (MPa)
5.54	1.08±0.10	not measured
7.47	1.10±0.04	12.92±4.47
8.46	2.04±0.27	5.14±1.40
9.46	3.75±0.86	10.10±3.59
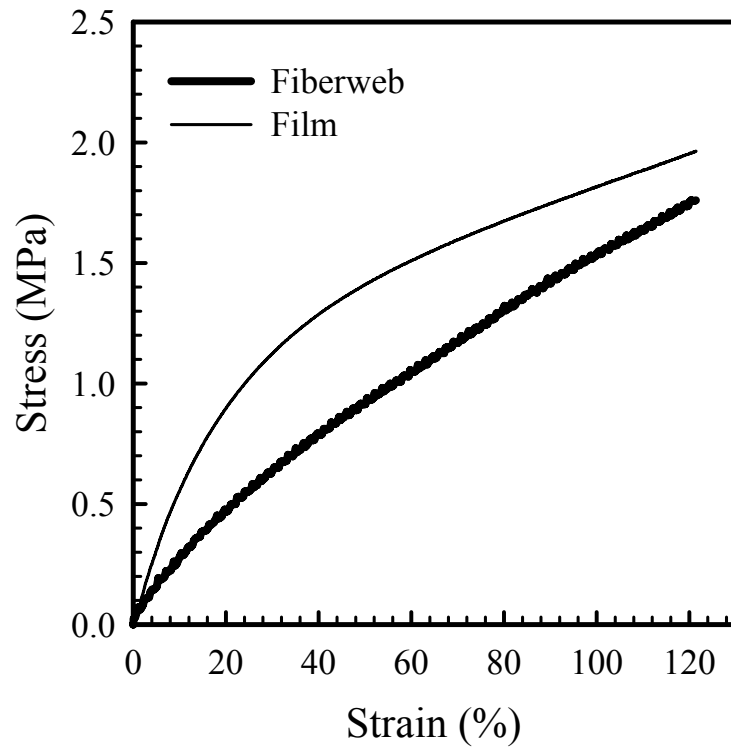
Figure 5.4. Tensile behavior of 8.46 vol% (nominal) carbon black filled films and fiberwebs. Modulus of the film is much higher than the fiberweb.

5.4.2. Piezoresistive Behavior

Fractional change in resistance as a function of applied strain for electrospun fiberwebs are shown in Figure 5.5 (a). Inset is the resistance change of fiberwebs. It is observed that the resistance of fiberwebs decreases until critical strain reached, and then increases over the critical strain. This trend is in agreement with previously reported behavior of polymer composites [19, 21, 35]. In general there are two competing phenomena of the resistivity change of conventional composite during elongation in a

composite system: the formation and destruction of conductive paths. At low strain, fillers can be reoriented along the strain direction, resulting in a decrease in the composite resistivity until the resistivity minimum reached. With increasing uniaxial strain, the increase of inter-particle distance and reorientation of particles can lead to a destruction of conductive network, leading to increase of the resistivity. This trend is also observed in the piezoresistivity behavior of the films in Figure 5.5 (b).

(a)
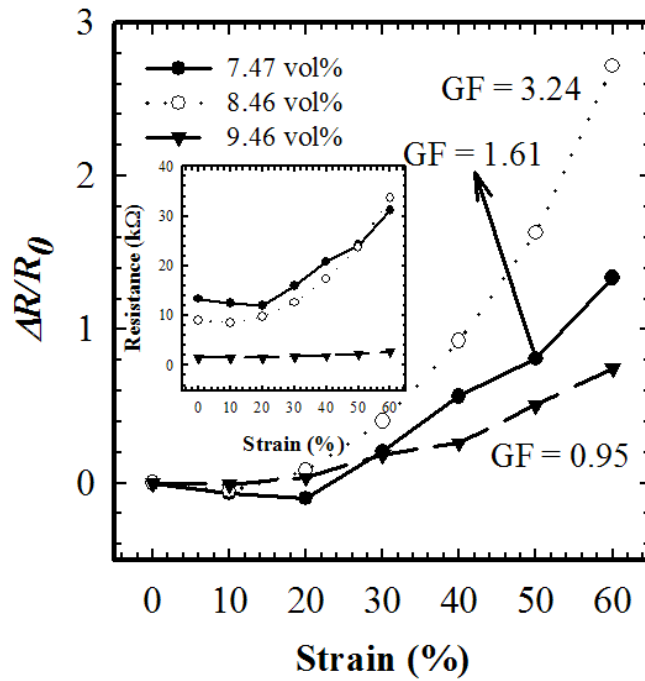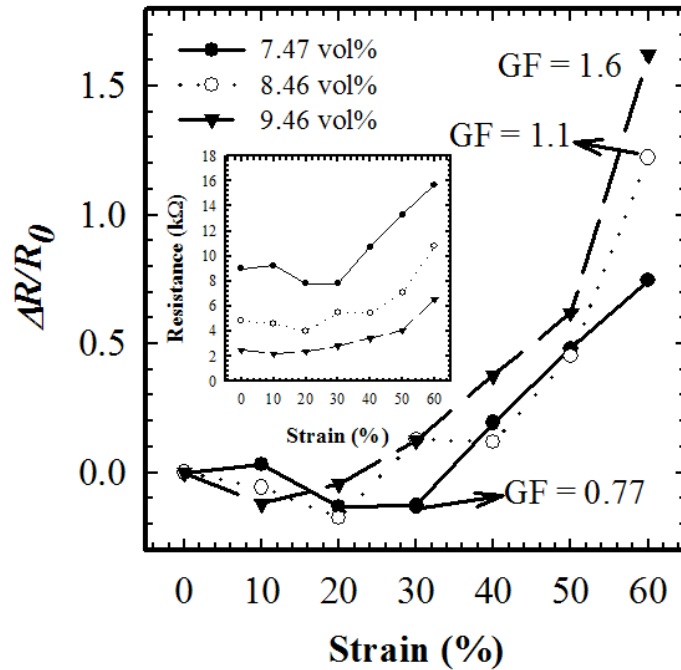
Figure 5.5. Piezoresistive behavior of electrospun (a) composite fiberwebs, and (b) spin cast films as strain increases up to 60%. Inset shows resistance change along the strain increase with a rate of 10% increase.

In the case of composite fiberweb, it consists of composite fibers. The decrease of fractional resistance change of fiberwebs at low strain seems to be more dominant by the increased fiber density and the fiber alignment with the applied strain than by the reorientation of the fillers. When a strain is applied to the electrospun polyurethane fiberwebs, fibers become oriented in the direction of strain applied and fiber density increases [36]. Therefore fiber contacts can be enhanced by the strain so that resistance

decreases at small deformation. At small deformation, the interfiber distance decreases with increasing applied strain and the formation of conductive paths is the predominant mechanism, resulting in a decrease in the fiberweb resistance until the resistance minimum is reached. Above critical strain, destruction of conductive paths dominates. This can be attributed to the filler reorientation in the fibers. When the fiberwebs are under stretching, carbon black particles bonded to the polymer chain are experienced to be stretched along the polymer chains and pulled apart each others. Also none bonded or agglomerated carbon black particles can be rearranged and separated over the tunneling distance. Hence resistance changes are increased like Figure 5.5. Reorientation of carbon black particles in the fibers may be more dominant effect of piezoresistive response of composite fiberweb than fiber realignments in the fiberweb at high strain.

The calculated GFs of bulk films range from 0.77 to 1.6 whereas fiberwebs range from 0.95 to 3.24. This value of gauge factor is relatively comparable to other system of composite such as carbon fiber reinforced polymer composite (GF: 2-6) [13, 37] or carbon black filled elastomer coated fabric based sensors (GF: 2.8) [38]. From this observation, fiberwebs are more efficient than the bulk films due to the higher aspect ratio and more deformability of fibers. In addition fiberwebs show high porosity up to

73%, indicating that higher piezoresistivity can be obtained with lower amount of solid

contents (filler and polymer) than films, see Table 5.2.

Table 5.2. Investigation of bulk density of fiberwebs and films and porosity of

fiberwebs.

Volume concentration of CB (nominal, vol%)	Bulk density of fiberweb (g/cm^3)	Bulk density of spin cast film (g/cm^3)	Porosity of fiberweb (%)
7.47	0.30	1.11	73.0
8.46	0.31	1.12	71.4
9.46	0.50	1.12	56.3

5.4.3. Actuation Response of Fiberwebs

Both high electrical conductivity and low initial modulus are necessary to generate

the high actuation. Electrospun carbon black filled composite fiberwebs exhibits high

conductivity up to 1.07×10^{-2} S/cm and initial modulus, 3.75 MPa. The actuation

response of the DEA based carbon black composite fiberweb and VHB film is shown in

Figure 5.6. When the high electric field is applied to the DEA, actuation response is

generated by the electrostatic force between two electrodes. Whereas electric field is off,

charge is not arranged by the dipole so that actuation response is gone. Actuation

response is calculated by the equation (5.2) and it is decreased with increasing carbon

black concentration. Maximum areal strain is around 12.74% from 5.58 vol% of carbon black filled electrodes. Figure 5.7 shows the actuation response of DEA with different concentrations of carbon black filled fiberweb electrodes. Increase of carbon black concentration lead to the decrease of areal strain. This may be related to the initial modulus of carbon black composite fiberwebs. The initial modulus of the composite fiberwebs increased with carbon black concentration from 1.10 to 3.75 MPa, see Table 5.1. In addition it is increased dramatically from 6.98 vol% of carbon black filled composite fiberweb, resulting in dramatic decrease of actuation response in spite of high electrical conductivity. Therefore the initial modulus of the electrode material is very important for the actuation response.

(a)   (b)
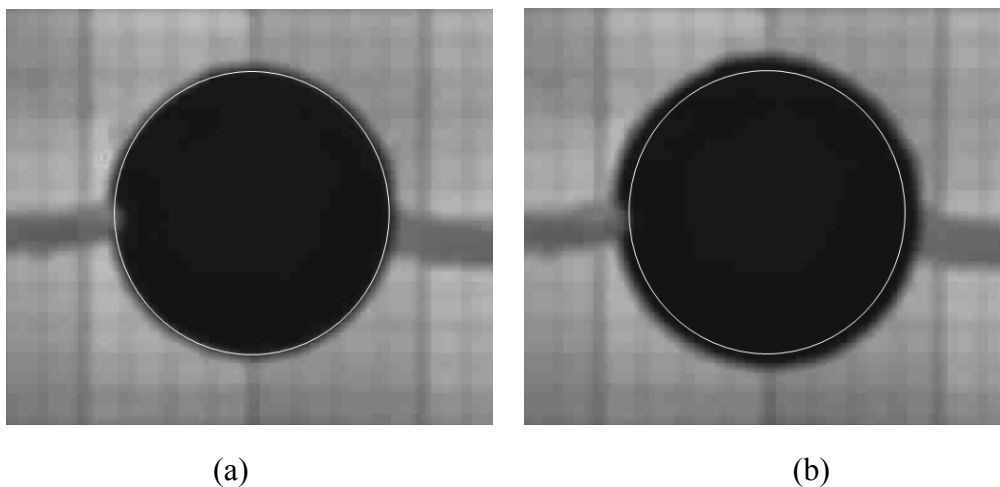
Figure 5.6. Actuation response of DEA consists of acrylic elastomer as a dielectric elastomer medium and electrospun 5.58 vol% CB-PU composite fiberweb as a flexible electrode: (a) voltage off, and (b) voltage on.
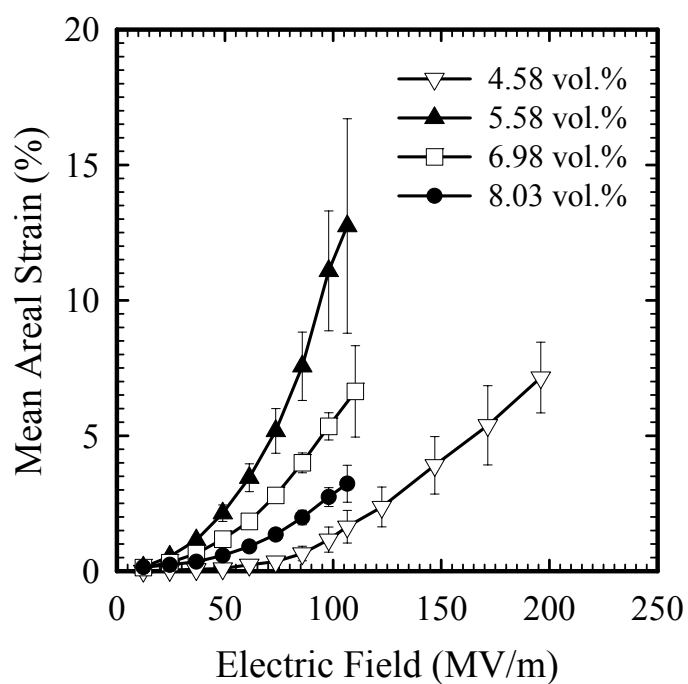

Figure 5.7. Actuation response of the DEAs consists of 4 different loadings of carbon black filled composite fiberwebs as electrodes and acrylic elastomer as a medium.

For the 4.58 vol% of carbon black filled composite fiberweb, its electrical conductivity is around 1.88×10^{-7} S/cm at low voltages. This would normally be considered an insulating material. However under the application of high voltages there appears to be sufficient fields to redistribute charge throughout the film either through dielectric breakdown between particles or tunneling/electron hopping processes. Thus even though the electrode appears to have low electrical conductivity at low voltages it shows 7% of actuation response. This confirms that actuation response of electroactive polymer actuators can be obtained with low electrical conductive electrode material when using high electric fields and Maxwell pressure. This is in agreement with Perline's published data using metallic compliant electrodes by depositing a gold traces in form of zig-zag on silicone elastomer [39]. In Perline's report, the low conductivity material limits breakdown current and localizes the breakdown effects to prevent breakdown of the actuator. From this fact, low conductive material can delay to pass the breakdown current. Therefore it shows the low and delayed actuation response like Figure 5.7.

5.5. Conclusions

We have successfully adapted the electrospinning technique to produce fiberweb based on CB-PU nanocomposite. Two important observations have to be pointed out in our present work. At first, fiberweb shows higher electrical conductivity and flexibility than the films. An CB-PU nanocomposite fiberweb and film were evaluated as an piezoresistive material and flexible electrode. It is observed that fiberwebs are more efficient than the films in terms of I-V characteristics, modulus, bulk density, and piezoresistivity. From the I-V curve, both materials show diode like behavior with little current for low voltages. However fiberwebs are more close to Ohmic behavior than the films. In terms of flexibility, elastic modulus of fiberwebs are much lower than the films. Moreover bulk density of films is 2-3 times bigger than bulk density of fiberweb. Thus fiberweb is more light, and more flexible, and better I-V characteristics than the films. In the case of piezoresistivity, both of materials show similar behavior, however gauge factor of fiberweb is little higher than the films. In second, CB-PU nanocomposite fiberweb was successfully applied in the form of flexible electrode of dielectric actuator. The maximum of mean areal strain was 12.74% with 5.58 vol% carbon black filled fiberweb. This may be due to the low modulus of materials combined with high

electrical conductivity. The results are showing a possible application of electrospun

composite fiberweb as a flexible electrode.

5.6 References

1. Xu, C.Y., Inai, R., Kotaki, M., and Ramakrishna, S., Biomaterials, 2004. **25**: p. 877.

2. Tsai PP, S.-G.H., Gibson P, *Different Electrostatic Methods for Making Electret Filters.* J Electrostatics, 2002. **54**: p. 333.

3. Kessick R, T.G., *Electrospun Polymer Composite Fiber Arrays for the Detection and Identification of Volatile Organic Compounds.* Sens Actuators, B, 2006. **Article in press**.

4. Ma M, M.Y., Gupta M, Gleason KK, Rutledge GC, *Superhydrophobic Fabrics Produced by Electrospinning and Chemical Vapor Deposition.* Macromolecules, 2005. **38**: p. 9742.

5. Kim, C., and Yang, K. S., *Electrochemical Properties of Carbon Nanofiber Web as an Electrode for Supercapacitor Prepared by Electrospinning.* Appl. Phys. Lett, 2003. **83**: p. 1216.

6. Ko, F., Gogotsi, Y., Ali, A., Naguib, N., Ye, H., Yang, G., Li, C., and Willis, P., *Electrospinning of Continuous Carbon Nanotube-Filled Nanofiber Yarns.* Adv. Mater., 2003. **15**(14): p. 1161.

7. Seoul, C., Kim, Y., and Baek, C., *Electrospinning of Poly(vinylidenefluoride)/Dimethylformamide Solutions with Carbon Nanotubes.* J Polym Sci, Part B: Polym Phys, 2003. **41**: p. 1572.

8. Pedicini, A., and Farris, R. J., *Thermally Induced Color Change in Electrospun Fiber Mats.* J Polym Sci, Part B: Polym Phys, 2004. **42**: p. 752.

9. Mazzoldi, A., De Rossi, D., Lorussi, F., Scilingo, E. P., and Paradiso, R., *Smart Textiles for Wearable Motion Capture Systems.* AUTEX R. J., 2002. **2**(4): p. 199.

10. Grimaldi, C., Ryser, P., and Strassler, S., *Piezoresistive Anisotropy of Thick-Film Resistors.* J. Eur. Ceram. Soc., 2004. **24**: p. 1893.

11. Grimaldi, C., Maeder, T., Ryser, P., and Strassler, S., *Critical Behavior of the Piezoresistive Response in RuO_2-Glass Composites.* J. Phys. D: Appl. Phys., 2003. **36**: p. 1341.

12. Wang, S., Kowalik, D. P., and Chung, D. D. L., *Self-Sensing Attained in Carbon-Fiber-Polymer -Matrix Structural Composites by Using the Interlaminar Interface as a Sensor.* Smart Mater. Struct., 2004. **13**: p. 570.

13. Todoroki, A., and Yoshida, J., *Electrical Resistance Change of Unidirectional CFRP Due to Applied Load.* JSME Int. J. Ser, A, 2004. **47**(3): p. 357.

14. Wu, Z.S., Yang, C. Q., Harada, T., and Ye, L. P., *Self-Diagnosis of Structures Strengthened with Hybrid Carbon-Fiber-Reinforced Polymer Sheets.* Smart Mater. Struct., 2005. **14**: p. S39.

15. Shui, X., and Chung, D. D. L., *A Piezoresistive Carbon Filament Polymer-Matrix Composite Strain Sensor.* Smart Mater. Struct., 1996. **5**: p. 243.

16. Chung, D.D.L., *Piezoresistive Cement-Based Materials for Strain Sensing.* J. INTEL. MAT. SYST. STR., 2002. **13**: p. 599.

17. Ogi, K., and Takao, Y., *Characterization of Piezoresistance Behavior in a CFRP Unidirectional Laminate.* Compos. Sci. Technol., 2005. **65**: p. 231.

18. Lu, J.W., Wang, W. L., Liao, K. L., and Wan, B. Y., *Strain-Induced Resistance Changes of Carbon Nanotube Films.* Int. J. Mod Phys B, 2005. **19**: p. 627.

19. Lu, J., Weng, W., Chen, X., Wu, D., and Chen, G., *Piezoresistive Materials from Directed Shear-Induced Assembly of Graphite Nanosheets in Polyethylene.* Adv. Funct. Mater., 2005. **15**: p. 1358.

20. Lu J, C.X., Lu W, Chen G, *The Piezoresistive Behaviors of Polyethylene/Foliated Graphite Nanocomposites.* Eur Polym J, 2006. **42**: p. 1015.

21. Flandin, L., Chang, A., Nazarenko, S., Hiltner, A., and Baer, E., *Effect of Strain on the Properties of an Ethylene–Octene Elastomer with Conductive Carbon Fillers.* J. Appl. Polym. Sci., 2000. **76**: p. 894.

22. Knite M, T.V., Kiploka A, Kaupuzs J, *Polyisoprene-Carbon Black Nanocomposites as Tensile Strain and Pressure Sensor Materials.* Sens Actuators, B, 2004. **110**: p. 142.

23. Zhang, X., Pan, Y., Zheng, Q., and Yi, XS, *Piezoresistance of Conductor Filled Insulator Composites.* Polym. Int., 2001. **50**: p. 229.

24. Jacq, C., Maeder, Th., and Ryser, P., *High-Strain Response of Piezoresistive Thick-Film Resistors on Titanium Alloy Substrates.* J. Eur. Ceram. Soc., 2004. **24**: p. 1897.

25. Gammelgaard, L., Rasmussen, P. A., Calleja, M., Vettiger, P., and Boisen, A., *Microfabricated Photoplastic Cantilever with Integrated Photoplastic/Carbon Based Piezoresistive Strain Sensor.* Appl. Phys. Lett, 2006. **88**: p. 113508.

26. Mallette JG, Q.L., Marquez A, Manero O, *Carbon Black-Filled PET/HDPE/ Blends: Effect of the CB Structure on Rheological and Electric Properties.* J Appl Polym Sci, 2001. **81**: p. 562.

27. Reneker DH, Y.A., Fong H, Koombhongse SJ, J Appl Phys, 2000. **87**: p. 4531.

28. Theron, S.A., Zussman, E., and Yarin, A. L., *Experimental Investigation of the Governing Parameters in the Electrospinning of Polymer Solutions.* Polymer, 2004. **45**: p. 2017.

29. Perline, R., Kornbluh, R., Kofod, G., *High-Strain Actuator Materials Based on Dielectric Elastomers.* Adv Mater, 2000. **12**: p. 1223.

30. Yamashita, Y., Tananka, A., Ko, F., *Charateristics of Elastomeric Nanofiber Membranes Produced by Electrospinning.* Rubber Expo Technical Meeting, 2003: p. 14.

31. Ounaies, Z., Park, C, Wise, K. E., Siochi, E. J., Harrison, J. S., *Electrical Properties of Single Wall Carbon Nanotube Reinforced Polyimide Composites.* Compos Sci and Technol, 2003. **63**: p. 1637.

32. Burkov, A.T., Vinzelberg, H., Schumann, J., Nakama, T., Yagasaki, K, *Strongly Nonlinear Electronic Transport in Cr-Si Composite Films.* J Appl Phys, 2004. **95**: p. 7903.

33. Balberg, I., *Tunneling and Nonuniversal Conductivity in Composite materials.* Phys. Rev. Lett., 1987. **59**(12): p. 1305.

34. Balberg, I., *A Comprehensive Picture of the Electrical Phenomena in Carbon Black–Polymer Composites.* Carbon, 2002. **40**: p. 139.

35. DAS NC, C.T., Khastgir D, *Effect of Axial Stretching on Electrical Resistivity of Short Carbon Fibre and Carbon Black Filled Conductive Rubber Composites.* Polym Int, 2002. **51**: p. 156.

36. Pedicini, A., and Farris, R. J., *Mechanical Behavior of Electrospun Polyurethane.* Polymer, 2003. **44**: p. 6857.

37. Gordon, D.A., Wang, S., Chung, D. D. L., *Piezoresistivity in Unidirectional Continuous Carbon Fiber Polymer-Matrix Composites: Single-Lamina Composite Versus Two-Lamina Composite.* Compos Interfaces, 2004. **11**: p. 95.

38. Tognetti, A., Lorussi, F., Tesconi, M., Rossi, D. D., *Strain Sensing Fabric Characterization.* IEEE Sensors Journal, 2004: p. 527.

39. Perline, R., Kornbluh, R., Joseph, J., Heydt, R., Pei, Q., and Chiba, S, *High-Field Deformation of Elastimeric Dielectrics for Actuators.* Mat. Sci Eng. C, 2000. **11**: p. 89.

CHAPTER 6. CONCLUSIONS

Carbon Black has been usually used as a conductive filler in rubbers or polymer composites, however its use as a conductive filler into the fiberweb has been limited. In our study, we have fabricated PU-CB composite fiberwebs using electrospinning and evaluated their electrical and mechanical characteristics. Limited comparison of the fiberweb behavior with comparable spin-cast films shows their relative advantages in certain key characteristics.

The percolation behavior of nanocomposite fibers filled with carbon black was simulated. Monte-Carlo method and Hoshen-Kopelman (HK) algorithm was successfully employed to simulate and analyze the random particle network in electrospun fiber matrix. Two types of lattices were employed: cubic type and super network type. As expected, the super network type shows lower percolation threshold than the square type due to higher probability to contact neighborhood carbon particles. Theoretically, the percolation threshold of the nanocomposite fiber filled with carbon black was determined to be around 9.3 vol%.

Electron micrographs revealed larger fiber diameters as well as higher bond density in fiberwebs with higher CB content. Significant improvement in certain mechanical

properties was achieved by the incorporation of carbon blacks. The initial modulus of the fiberweb increased substantially with increasing CB content. The increase in bond density and the over-all area of the bonds for higher CB content as well as the reinforcement effect of high modulus CB particles are likely to improve the modulus of the fiberweb. The presence of CB increased fiberweb strength marginally up to 3.65 vol% (nominal) of CB content and fell significantly beyond that. Thermal stability of CB-PU composite fiberweb increased significantly up to 5.54 vol% (nominal) of carbon black loadings and dropped beyond that. The reason for lowering of thermal stability at higher CB loadings is not clear. However it could be due to the agglomeration of CB at higher loadings. The electrical conductivity of the composite fiberweb was found to increase about 3 orders of magnitude when the filler content increased from 4.58 vol% to 4.92 vol%. The percolation threshold of conductivity was determined to be between 4.58-4.92 vol% of CB. The critical exponent of percolation (t) was calculated as 2.165, when the percolation threshold was assumed to be around 4.6 vol%. Electrical conductivity values for fiberwebs were generally higher than comparable spin-cast films. This may be due to the higher surface area of fiberwebs than the films and the difference in CB particle distribution within the matrix. Studies of current-voltage relationship of the fiberwebs seem to confirm the tunneling-percolation behavior of the

CB-PU composite fiberweb investigated in this research. Piezoresitive behavior of the electrospun fiberwebs was found to be comparable to equivalent spin-cast films. Gauge-factor values of electrospun fiberwebs were determined to be in the range of 1.6 to 3.24. The CB-PU nanocomposite fiberweb was successfully applied in the form of flexible electrodes on a circular dielectric elastomer actuator. The maximum mean areal actuation strain of 12.74% was recorded with 5.58 vol% carbon black filled fiberweb as electrodes applied on and VHB-4910 acrylic films.

In summary, the potential of PU-CB composites as flexible and porous electrically conductive substrates has been demonstrated. However, further assessment of the material is needed to improve the fabrication process and behavior.

APPENDICES

A. Hoshen and Kopelman (HK) Algorithm

The percolation system consists of randomly distributed conducting and isolating sites. When the fraction of the conducting sites exceeds a percolation threshold, spanning clusters will be formed in the matrix. If the media is quiet big, it is not easy to analysis the structure of the clusters in percolation phenomena. For example, distinguish that the cluster belongs to spanning cluster is one of difficult problems. The introduction of the Hoshen and Kopelman algorithm [1] improved this difficulty in percolation. HK algorithm is mainly based on the application of alternate labels to sites belonging to the same cluster. If the two neighboring sites are occupied and have different labels, minimum label between neighboring sites is assigned to the neighboring sites. For example, site (4,3) in Figure A.1 (a) is improper cluster labels because it is connected to the cluster which is labeled 1. It is modified properly in Figure 7.1 (b).

1	1	0	0	2
1	0	3	0	0
1	0	0	4	4
1	1	1	1	0
1	0	0	1	1

1	1	0	0	2
1	0	3	0	0
1	0	0	1	1
1	1	1	1	0
1	0	0	1	1

(a) Improper labeling   (b) proper labeling

Figure A.1. A percolation configuration of a square lattice.

After the introduction of HK algorithm, Monte Carlo simulations of very large size of the system become possible and HK algorithm has been further extended to determine information not only on the cluster size but also on the structure of the clusters [2, 3].

B. Measurement of Electrical Resistivity of Electrospun Composite Fiberwebs

The electrical resistances of the nanocomposite fiberwebs were measured by the four-point probe technique. A four point probe instrument, consists of Keithley 220 current source and a Keithley 6517A electrometer, was used to measure the current-voltage characteristics of the samples. Each sample was prepared in the dimension of 10 cm length and 4 cm width. The average resistance value of each specimen was obtained from 30 repeated measurements at various positions of the sample. With the measured resistance and sample geometry, electrical resistivity was calculated using the equation below

$$\rho = 4.532t\left(\frac{V}{I}\right)$$

(7.1)

where V is a voltage, I is a current applied, and t is the thickness of the sample. The

conductivity (σ)is a reciprocal of equation (7.1).

$$\sigma = \frac{1}{\rho}$$

(7.2)

C. Measurement of Thickness of CB-PU Electrospun Fiberwebs

The thickness of CB-PU electrospun fiberweb was measured using micrometer (L&W model 51, 7.3 ±0.3 psi).   Measurement was done by following TAPPI 411-om-89 method. The average thickness value of each specimen was obtained from 50 repeated measurements at various positions of the sample. Figure C.2 shows the thickness of electrospun CB-PU composite fiberweb increases with increasing of CB loadings.
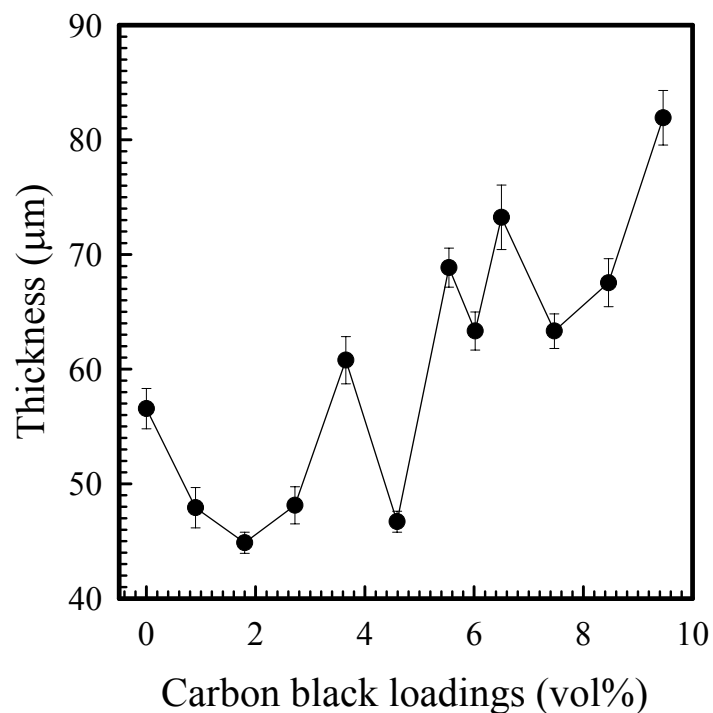
Figure C.2. Thickness of various loadings of CB-PU electrospun fiberweb. The error

bars correspond to 95% confidence intervals.

D. Measurement of Particle Size Distribution on the 7.47 vol% (nominal) CB-PU

by Optical Microscope

To assess the level of dispersion, the solutions prepared for electrospinning were

evaluated in terms of the dispersed particle size using an optical microscope (Olympus

BX 60 with PAX-it-M1243 Modulator 20 X software). Particle diameter was measured

from microscopic image using image analysis software (Image J ver. 1.34s). The

measurement of particle size was based on the diameter of particles from 100 different

random locations. Figure D.3 shows histogram of particle size distribution in 7.47 vol% (nominal) of CB filled solution before electrospinning. Limited analysis of the optical images show aggregate size in the range of 200-1700 nm, mean diameter is 430 nm.
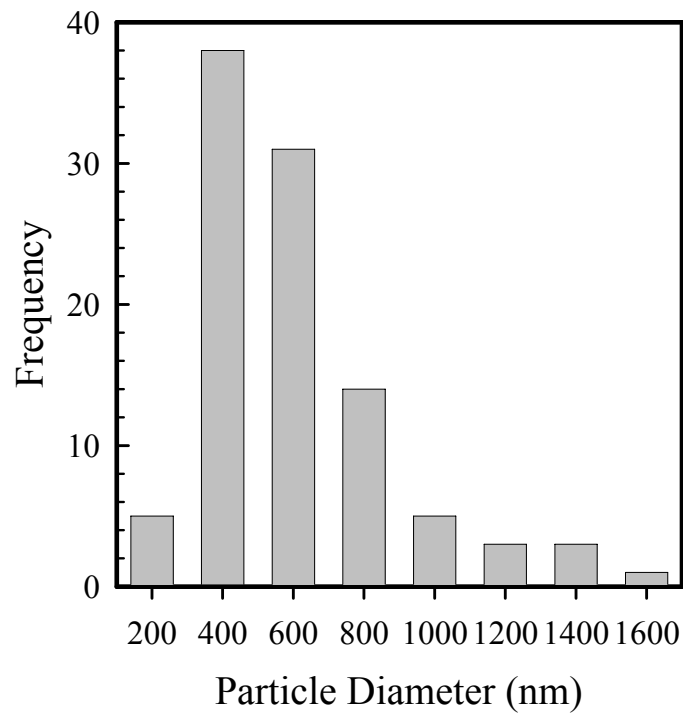

Figure D.3. Particle size distribution of 7.47vol% (nominal) CB-PU solution by optical microscope.

E. References

1.   Hoshen, J., and Kopelman, R., Phys. Rev. B, 1976. **14**: p. 3438.

2.   J. Hoshen, a.M.W.B., and K. S. Miner, Phys. Rev. B, 1997. **56**(1455).

3.   A. Al-Futisi, a.T.W.P., Physica A, 2003. **321**: p. 665.